Indonesian Journal of Modern Science and Technology Modern (IJMST)
Vol. 1, No. 3, September 2025, pp. 89-114
E-ISSN: 3090-3831 | DOI: doi.org/10.64021/ijmst.1.3.88-113.2025

Mathematical Modelling of Endosulfan Adsorption Using Activated and Unactivated Boiler Fly Ash and Maize Cob

Osu Bright O [1,3*], Igwe J.C [2,4], Olunkwa C. [1,3], Aghalibe C.U [2], Onwuka, K.E [2]
[1] Department of Mathematics, Abia State University Uturu, 460101 Nigeria
[2] Department of Pure and Industrial Chemistry, Abia State University Uturu, 460101 Nigeria
[3] Department of Mathematics, Kingsley Ozumba Mbadiwe University, Ideato, Imo State Nigeria
[4] Department of Chemistry, Kingsley Ozumba Mbadiwe University, Ideato, Imo State Nigeria

ARTICLE INFO

Article history:

Received June 8, 2025
Revised September 20, 2025
Published September 27, 2025

Keywords:

Agricultural by-products;
Contamination; Isotherm; Pesticides,
Toxic compounds;

ABSTRACT

The application of pesticides to control plant pests and increase yield introduces issues of pesticide contamination and toxicity. Endosulfan, a persistent organic pollutant, poses serious ecological and public health risks due to its toxicity, persistence, and bioaccumulative nature. Conventional remediation methods are often costly and generate secondary waste, hence the need for sustainable, low-cost alternatives. This work investigated the mathematical modelling of endosulfan adsorption from aqueous solutions using activated and unactivated boiler fly ash and maize cob. Batch adsorption experiments were conducted to examine the effects of contact time, initial concentration, and activation of adsorbents. The behavior of pesticide adsorption data against certain isotherm and kinetic equations was also investigated. The physicochemical properties of the activated and unactivated maize cob and boiler fly ash, as well as FT-IR, XRD, and SEM of the adsorbents, were determined. Both initial pesticide concentration and contact time affected the adsorption capacity of the adsorbents. As the initial concentration increased, the amount of pesticide adsorbed also increased. An increase in contact time rapidly increased the amount adsorbed until it reached a maximum at 60 minutes, after which it decreased; hence, equilibrium was reached after 60 minutes. Activation enhanced the porosity, cation exchange capacity, and surface functional groups of the adsorbents. Activated maize cob exhibited the highest adsorption capacity, followed by activated boiler fly ash, while unactivated forms showed comparatively lower performance. Equilibrium data fitted best to multilayer and heterogeneous surface models, while kinetic analysis suggested chemisorption tendencies. Activated maize cob and boiler fly ash are effective, eco-friendly, and low-cost adsorbents for the removal of endosulfan from aqueous systems. Mathematical modelling provided predictive insights into adsorption behavior, supporting process optimization. The findings demonstrate the potential of agricultural and industrial residues as sustainable alternatives for pesticide remediation and environmental protection.

Corresponding Author:

Coresponding: Osu Bright O, Department of Mathematics, Abia State University Uturu, 460101 Nigeria.
Email: osu.bright@abiastateuniversity.edu.ng

1. INTRODUCTION

Globally, the immense pressure exerted by the industrial activities on natural resources has resulted into industrialization, urbanization and environmental pollution problems which affect its exploration and utilization. As a result of these adverse effects of pollution problems that emanate from the discharge of untreated industrial waste into the environment, agricultural activities and every living thing are faced with serious ecological and public health risks due to its toxicity, persistence, and bioaccumulative nature of organic pollutant. Analysis has shown that while the world's population is on the increase, the need to increase food production and its preservation with the use of hydrophobic and persistent pesticides increases and this require the application of pesticides such as endosulfan, to control pests for increased crop yield. The widespread use of pesticides in modern agriculture has raised significant environmental and public health concerns due to their persistence, toxicity, and tendency to accumulate in ecosystems. Among these challenges, endosulfan, a chlorinated cyclodiene pesticide, which has been classified as a persistent organic pesticide with best adsorption behaviour and non-toxic [1], has attracted global attention because of its long environmental benefits, and potential to bioaccumulate in soil and water systems [2].

Endosulfan is recognized as a commonly applied agricultural pesticide, extensively used worldwide as a broad-spectrum insecticide on crops such as cotton, tea, sugarcane, vegetables, and fruits [3]. Despite being banned recently or severely restricted in many countries under the Stockholm Convention, it has been reported that residues of previously used endosulfan, are still detected in agricultural soils and water bodies, especially in developing nations where regulation and monitoring are limited [4][5][6], causing various toxicity problems and affecting farm lands, hence, affecting food security [7]. Therefore, the contamination of aquatic ecosystems by endosulfan poses risks not only to aquatic organisms but also to human populations through the food chain and drinking water supplies [2].

Environmental pollution and toxicity problems caused by pesticides such as Endosulfan have been well reported [8][9][7][5][10][11]. To address these risks, numerous techniques have been developed to remove pesticide contaminants from aqueous solutions, including leaching, chromatography, volatilization, precipitation, ozonation, hydrostatic pressure, and adsorption, thereby ensuring effective decontamination [12][13]. But effective and sustainable methods for pesticide removal from aqueous solutions are urgently needed. Conventional treatment methods such as advanced oxidation processes, chemical precipitation, and membrane filtration are often costly, energy-intensive, and generate secondary pollutants [14]. Many pesticides exhibit strong affinity for soil particles; consequently, their high sorption capacity, low water solubility, and low vapor pressure render leaching, precipitation, and volatilization insignificant pathways for pesticide dissipation.

Adsorption has been widely reported as a key unit operation in waste decontamination and is regarded as a highly effective technique, wherein contaminants adhere to the surface of an adsorbent, enabling their removal from wastewater [15][10]. Moreover, adsorption is a critical factor influencing the environmental fate of pesticides in soil, as it governs their distribution between soil and aqueous phases [8]. Therefore, adsorption technology has emerged as a simple, economical, and efficient approach for removing persistent organic pollutants from water [16][17]. The choice of adsorbent is critical, with increasing emphasis on low-cost, eco-friendly alternatives derived from agricultural and industrial residues. Activated carbon has been employed in the adsorption of pesticides from aqueous solution but conventional activated carbon adsorption has been reported to be very expensive [18]. Hence, the search for low cost, readily available agricultural by-products such as maize cob and boiler fly ash for pesticide decontamination, hence, conversion of waste to wealth.

Boiler fly ash (BFA), an industrial by-product from palm oil mills, thermal power plants, etc., is rich in silica, alumina, and carbon, making it a promising material for adsorption applications. However, its adsorption capacity is often limited by surface characteristics, necessitating activation treatments such as chemical or thermal modification to enhance porosity and functional groups [19]. Similarly, maize cob, an abundant lignocellulosic agricultural waste in many parts of Africa and Asia, has been recognized as a sustainable bio-adsorbent precursor. When activated, maize cob biomass develops functional oxygen-containing groups and a high surface area that can improve pesticide uptake [20].

Mathematical modelling of adsorption processes is essential for understanding adsorption mechanisms, designing treatment systems, and predicting performance under varying conditions. Models such as the Langmuir and Freundlich isotherms describe equilibrium behaviour, while pseudo-first order and pseudo-second-order kinetics explain adsorption rates. Applying these models to endosulfan adsorption onto activated and unactivated BFA and maize cob is crucial for assessing their potential as sustainable adsorbents for pesticide remediation.

Therefore, in this research, the adsorption of Endosulfan pesticide using boiler fly ash and maize cob was studied. The effects of adsorption contact time, initial concentration of pesticides, and activation of the

adsorbents were investigated. Comparison of the sorption capacity of the adsorbents was investigated, and the experimental results were fitted to some isotherm and kinetic models. By integrating experimental adsorption studies with mathematical linear models of the adsorption isotherms, this research aims to evaluate the efficiency, mechanisms, and feasibility of these low-cost adsorbents for environmental remediation of pesticides. Therefore, this study will serve as a cost effective, as well as an environmental sound alternative to the conventional methods of pesticides decontamination and elucidate on the fitness of the models to the sorption data for mathematical model predictive studies. Although several studies have examined adsorption of pesticides on natural and synthetic adsorbents, limited attention has been given to the comparative evaluation of activated and unactivated industrial and agricultural wastes such as BFA and maize cob. Moreover, the integration of comprehensive mathematical models-covering equilibrium studies-remains underexplored for endosulfan removal. Addressing this gap will provide a deeper understanding of adsorption mechanisms and support the development of low-cost, sustainable treatment technologies

2. METHODS

2.1. Materials

Boiler fly ash was obtained from Palm oil mill located at Uturu, Abia state, while maize cob was obtained from a refuse dump site at Eke market Okigwe, Imo State Nigeria. All reagents used were of analytical grade, purchased and used without further purification. Instakill Endosulfan pesticide (C9H6Cl6O3S),(6,7,8,9,10-hexachloro-1,5,5a,6,9,9a-hexahydro-6,9-methano-2,3,4-benzodioxathiepin-3-oxide), 350g/L, manufactured by Zibo Nab Agrochemicals Ltd China was purchased and used without further purification. The chemical structure of the endosulfan pesticide is presented in Figure 1 [11], and its physicochemical properties are summarized in Table 1. Doubly distilled–deionized water was employed for all dissolution and dilution procedures.

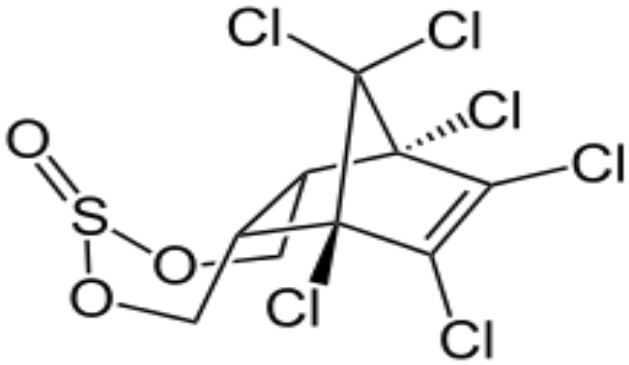

Fig. 1. Chemical structure of Endosulfan pesticide

Table 1. Properties of Endosulfan pesticide

Chemical formula	**Molar mass**	**Appearance**	**Odour**	**Density**
$C_9H_6Cl_6O_3S$	406.90 g·mol^{-1}	Brown crystals	Slight sulphur dioxide odour	1.745 g/cm^3
Melting point	Boiling point	Solubility in water	Vapour pressure	
70 to 100 °C	Decomposes	0.33 mg/L	0.00001 mmHg (25 °C)	

2.2. Method

The linear forms of mathematical adsorption kinetics and intraparticle diffusion model equations were used for the analysis of this study to determine the absorption diffusion rate of endosulfan pesticide on the prepared adsorbents and adsorbates of maize cob and boiler fly ash. Also, Mathematical isotherm models to determine the adsorption equilibrium data. The maize cob was thoroughly washed with tap water followed by deionized water, ground into a powdered form, and air-dried. Large agglomerates present in the boiler fly ash were removed, after which both the maize cob and boiler fly ash were sieved using a test sieve shaker (EFL

IMK3 model, Endecott's, England). The fraction retained on the 250 µm sieve was selected for use. Each adsorbent was divided into two portions. One portion was treated with 2% (v/v) nitric acid for 24 h, followed by filtration and air-drying; these samples were designated as activated boiler fly ash (ABFA) and activated maize cob (AMC) for experimental analysis. The remaining portions were left untreated and designated as unactivated boiler fly ash (UBFA) and unactivated maize cob (UMC). Some portions were used to characterize the adsorbent, using FT-IR, XRD, SEM and other physicochemical characteristics.

Stock solutions of endosulfan with known concentrations were prepared and working solutions of varying concentrations were obtained through serial dilution. The concentration of endosulfan remaining in solution after adsorption was determined using a UV–Vis spectrophotometer operating in the 200–960 nm wavelength range. Residual endosulfan concentrations were quantified using a calibration curve constructed in accordance with the Beer–Lambert law.

2.3. Effect of initial concentration

About 100 mL of different concentrations (10 mg/L to 100mg/L) of Endosulfan pesticide solutions were put in reagent bottles and 1.0 g each of ABFA, UBFA, AMC and UMC of 250 µm size were separately added to different reaction mixtures and agitated in a constant temperature rotary shaker at 100 rpm, temperature of 30°C and pH of 7.5 for 1 hr. After 1 hr, the reaction mixtures were centrifuged, and the supernatants were filtered rapidly through a Whatman No. 41 filter paper. The pesticide concentration in the filtrate was determined using a UV-vis absorption spectrophotometer model SP-300.

2.4. Effect of Contact Time

Batch absorption experiments were performed at various time intervals. 100 mL of Endosulfan pesticide solution concentration of 100 mg/L were put in reagent bottles and 1.0g each of ABFA, UBFA, AMC and UMC of 250 µm size were separately added to the different solution mixtures and were monitored in a constant temperature rotary shaker for different time intervals (10 mins to 120 mins), at a constant temperature of 30°C and pH of 7.5. After the required time interval, the reaction mixture was centrifuged, and the supernatant was filtered rapidly through a Whatman No. 41 filter paper. The pesticide concentration in the filtrate was determined using a UV-vis absorption spectrophotometer model SP-300.

3. RESULTS AND DISCUSSION

The linear forms of mathematical adsorption kinetics and intraparticle diffusion model equations used for this study are pseudo-first order [21] (Eq. 14 below), pseudo-second order [22] (Eq. 15 below), Ritchie's second order [23] (Eq. 16 below), for adsorption kinetics; Penetrant transport equation (Eq. 17 below) Elovich equation (Eq. 18 below), and McKay and Poots (Eq. 19 below) equations [24][25][26] to determine the adsorption behaviour of Endosulfan over other hydrophobic and persistent pesticides. Endosulfan adsorption behaviour does not occur at the surface alone but also involves gradual penetration into the pores of the adsorbent. This behaviour is best described by the intra-particle diffusion, which evaluates diffusional relationships and differences of Endosulfan pestcide into the internal pores of the adsorbent without the rate-limiting step. The amount of Endosulfan pesticide adsorbed for each of the parameters; initial concentration and contact time were plotted to find the variation in the adsorption capacity for the effect of the parameters. Adsorption isotherms, kinetic and intraparticle diffusion equations were used to treat the adsorption date to obtain various important interpretation of the adsorption process. Mathematical isotherm models as stated in equations 1, 2,3,4,5 and 6 were also applied to determine the adsorption equilibrium data. The analysis of the obtained adsorption data using the applied mathematical models as stated in literature are presented in tabular and graphical forms below.

3.1. Adsorbent Characterization

The results of the physicochemical properties of the activated boiler fly ash (Act-BFA), activated maize cob (Act-MC), unactivated boiler fly as (Unact-BFA) and unactivated maize cob (Unact-MC) are presented in Table 1. The results of the FT-IR, XRD and SEM are shown in Figure 2, Figure 3, Figure 4 and Figure 5 respectively.

Table 1. Physicochemical properties of unactivated and activated maize cob and boiler fly ash

Adsorbent	Ash Content (%)	Bulk Density (g/ml)	Pore Density (Porosity)	Pore Volume	Cation Exchange Capacity (CEC) (cmol/kg)	Electrical Conductivity (EC) (us/cm)
Unact-MC	4.210	0.068	0.932	46.6	0.072	103.200
Act-MC	4.773	0.042	0.958	47.9	0.097	89.132
Unact-BFA	5.211	0.144	0.856	42.8	0.024	84.712
Act-BFA	5.624	0.075	0.925	46.25	0.075	91.421

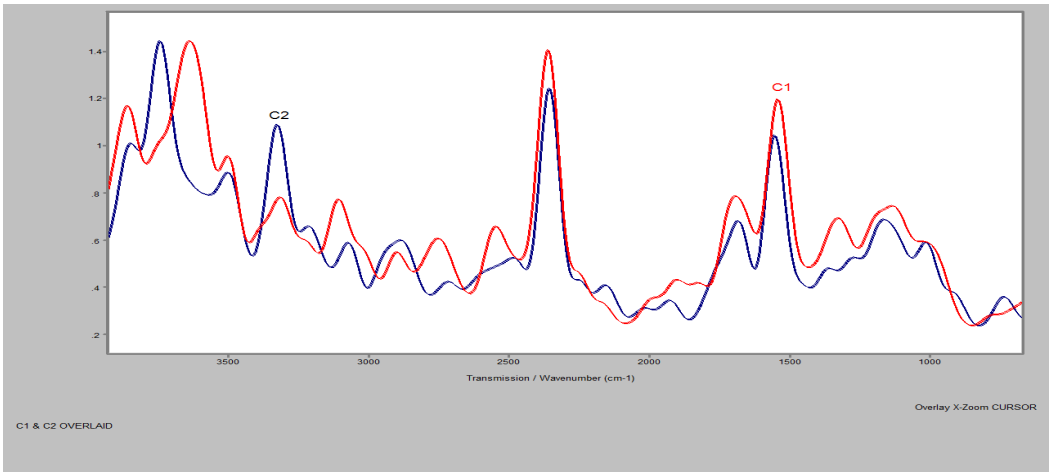

Fig. 2. FT-IR spectra of Unact-MC (C1) and Act-MC (C2)

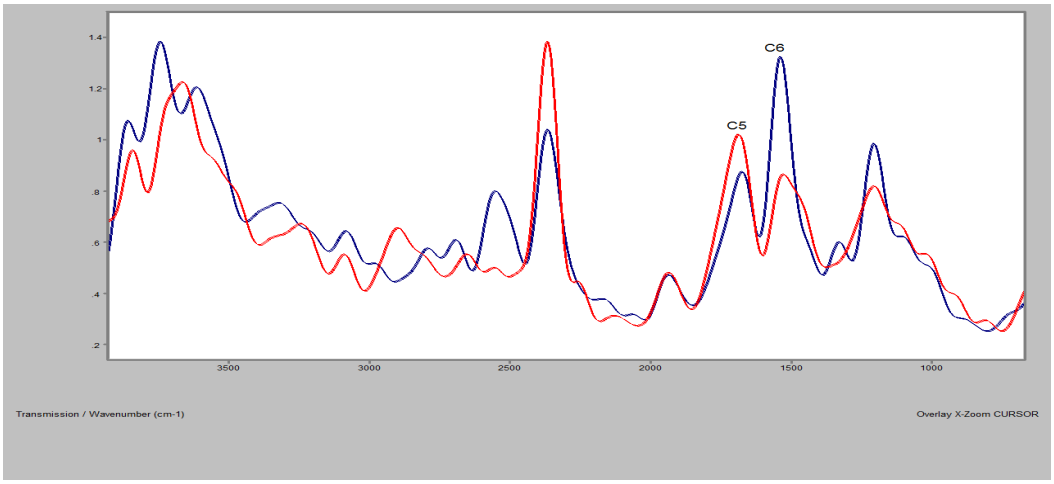

Fig. 3. FT-IR spectra of Unact-BFA(C5) and Act-BFA (C6) for adsorption of endosulfan

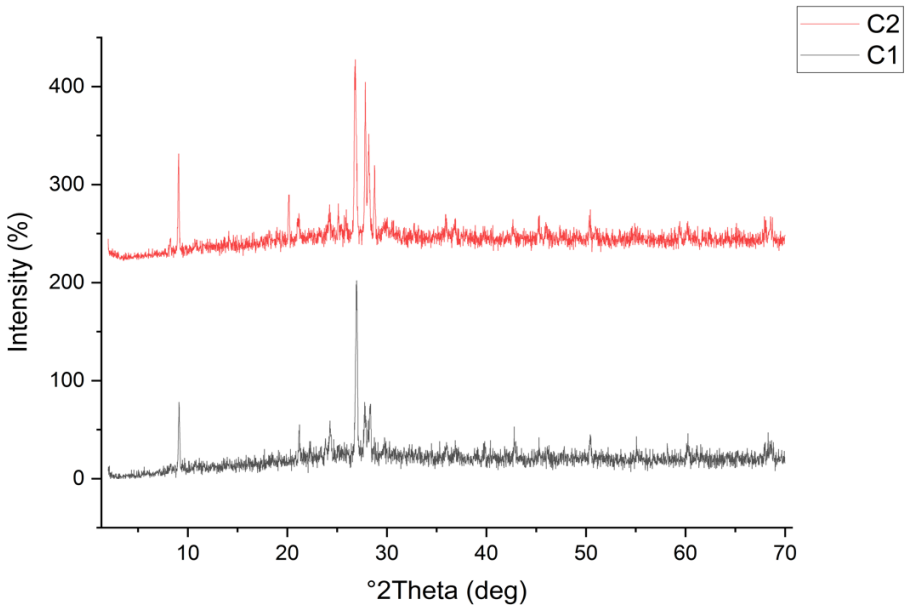

Fig. 4. XRD spectra of Unact-MC (C1) and Act-MC (C2)

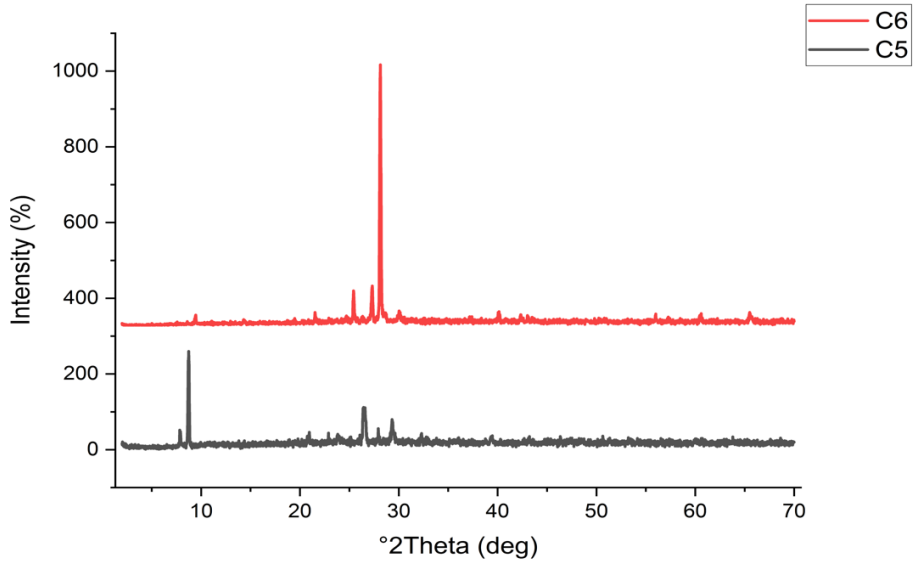

Fig. 5. XRD spectra of Unact-BFA(C5) and Act-BFA (C6) for adsorption of endosulfan

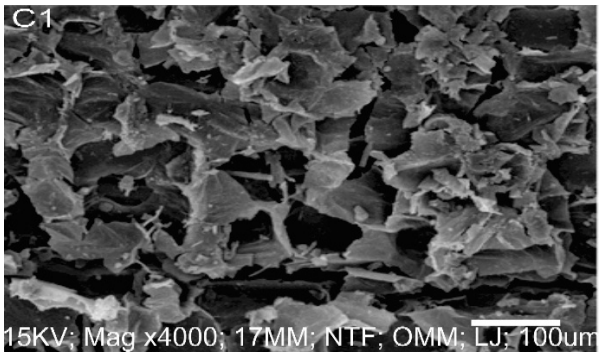

Fig. 5. SEM spectra of (C1) Unact-MC for adsorption of endosulfan

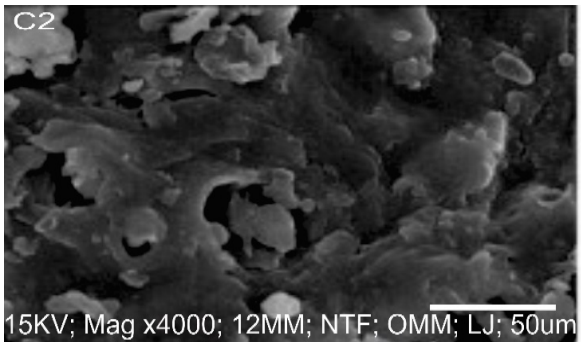

Fig. 6. SEM spectra of (C2) Act-MC for adsorption of endosulfan

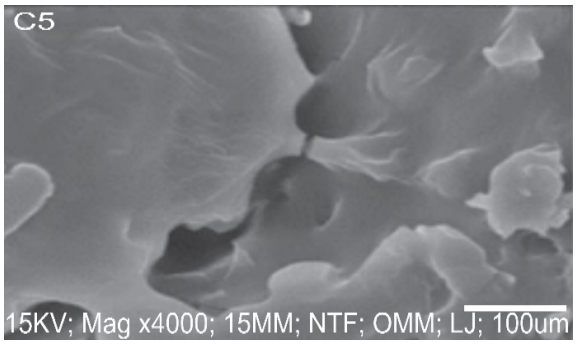

Fig. 7. SEM spectra of (C5) Unact-BFA for adsorption of endosulfan

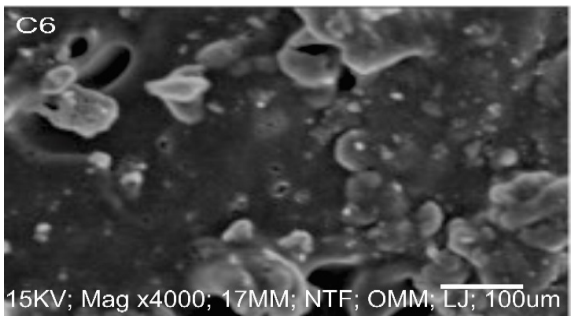

Fig. 7. SEM spectra of (C6) Act-BFA for adsorption of endosulfan

Ash content slightly increased after activation for both adsorbents; Unact-MC (4.210%); Act-MC (4.773%) and Unact-BFA (5.211%), Act-BFA (5.624%). This implies that the activation process enhanced the concentration of inorganic constituents. The increase may be due to the removal of volatile organic matter during activation, leaving behind more stable inorganic residues. High ash content is beneficial for adsorption. Bulk density decreased with activation for both adsorbents; Unact-MC (0.068), Act-MC (0.042), Unact-BFA (0.144), Act-BFA (0.075), indicating that the activation process made the structure lighter and more porous, which is consistent with the development of internal pore networks. A lower bulk density generally implies higher surface area per unit mass, which enhances adsorption capacity.

Activation increased porosity in both adsorbents. This confirms that activation treatments successfully opened more pores, improving accessibility for adsorbate molecules. Higher porosity means improved diffusion and adsorption efficiency. Also, the pore volume increased after activation, further demonstrating that activation created more pores and channels in the adsorbents. More pesticide molecules are accommodated at higher pore volume. CEC increased significantly after activation. This is critical because higher CEC means more sites are available for ion exchange, which strengthens the adsorbent's ability to bind cationic species and polar pesticide molecules. The improvement in BFA is particularly striking; suggesting activation strongly enhanced its surface functional groups. Electrical conductivity (EC) decreased slightly for maize cob but increased for boiler fly ash after activation. A decrease in EC for maize cob may indicate partial removal of soluble salts during activation. In contrast, the increase for BFA suggests exposure of mineral salts or oxides

with ionic mobility. EC values reflect the presence of soluble inorganic ions, which can influence adsorbent–adsorbate interactions.

Activation improved the surface and structural properties (porosity, pore volume, CEC) of both adsorbents, making them more effective for adsorption. Maize cob (MC), both unactivated and activated, shows lower ash content and bulk density but higher porosity compared to BFA, suggesting it is more lightweight and potentially better suited for organic pesticide adsorption. Boiler fly ash (BFA) has higher ash content and bulk density but, after activation, shows remarkable improvement in porosity and CEC, making it competitive as an adsorbent. Generally, the activation process enhanced the adsorptive potential of both maize cob and boiler fly ash by increasing porosity, pore volume, and CEC, while modifying their bulk density and conductivity, which are key for adsorption performance.

The FTIR spectra of the adsorbents revealed the presence of surface functional groups that play critical roles in Endosulfan adsorption. A broad band around 3400 cm^{-1} corresponded to –OH stretching vibrations of hydroxyl groups from cellulose and hemicellulose groups, which can form hydrogen bonds with the electronegative atoms in Endosulfan molecules (e.g., oxygen in the sulfone group). Peaks near 2920–2850 cm^{-1} were attributed to aliphatic C–H stretching, while a distinct band at ~1630–1650 cm^{-1} indicated C=O stretching vibrations of carboxyl and carbonyl groups that can interact with Endosulfan through dipole–dipole forces. Strong bands observed in the region of 1000–1100 cm^{-1} represented Si–O–Si and C–O stretching, which may also participate in adsorption through electrostatic interactions. After activation, the intensities of O–H and C=O bands increased, reflecting the exposure of more surface functional groups.

SEM micrographs provided evidence of morphological transformations induced by activation and adsorption. The unactivated adsorbents showed relatively smooth and compact surfaces with limited pore structures, which restrict adsorption efficiency. Activated maize cob and boiler fly ash, on the other hand, exhibited highly porous, fractured, and heterogeneous surfaces, with numerous cavities and channels that enhance accessibility for pesticide molecules. These morphological observations corroborate the improved adsorption capacities recorded in equilibrium experiments.

XRD analysis revealed differences in structural characteristics between maize cob and boiler fly ash. For maize cob, XRD analysis confirmed its largely amorphous structure, which is beneficial for endosulfan adsorption due to greater surface defects and disordered regions that promote π–π interactions with the aromatic rings of endosulfan. In contrast, boiler fly ash displayed sharp diffraction peaks corresponding to crystalline silica (SiO_2) and alumina (Al_2O_3), indicating a mineral-rich composition. These crystalline oxides can participate in surface complexation and electrostatic interactions with the polar functional groups of endosulfan. Activation resulted in reduced peak intensities and slight broadening of amorphous regions, reflecting structural modification and increased active surface sites.

The complementary results from FTIR, SEM, and XRD analyses confirm that activation significantly enhances the adsorption capacity of maize cob and boiler fly ash for Endosulfan by (i) exposing more active functional groups, (ii) enhancing surface roughness and porosity, and (iii) introducing structural modifications that increased surface defects. FTIR confirmed the functional groups responsible for binding, via hydrogen bonding, hydrophobic effects, and surface complexation. SEM showed the development of rough, porous surfaces that facilitated greater pesticide uptake, while post-adsorption images confirmed surface coverage by endosulfan. XRD highlighted the contributions of both amorphous phases (in maize cob) and crystalline mineral phases (in boiler fly ash) to the adsorption process. The amorphous structure of maize cob favoured π–π interactions with the aromatic components of endosulfan, while the mineral phases in fly ash supported electrostatic binding. Together, these findings provide strong evidence that surface chemistry, morphology, and structural phases work synergistically to improve endosulfan adsorption after activation.

3.2. Effect of Initial Pesticide Concentration

The effect of varying initial concentration of pesticide solutions is very important because this will help to show how initial concentration of pesticides solution affects the adsorption of the pesticides by the adsorbents. The result of the effect of varying initial concentration of Endosulfan is shown in Figure 8.

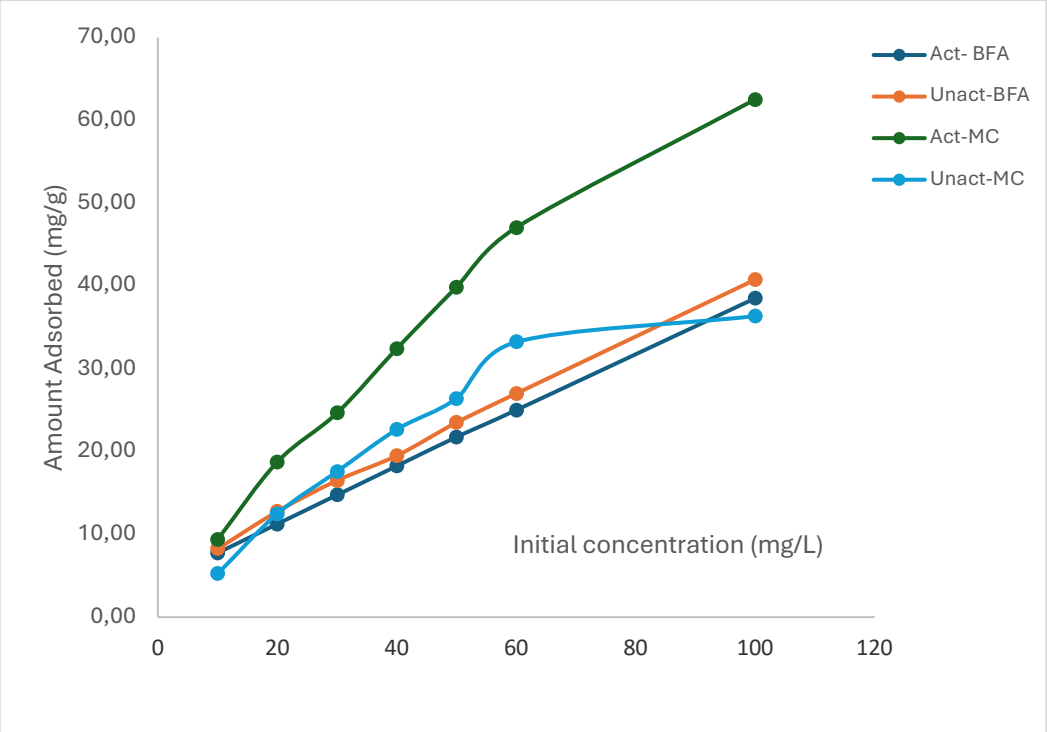

Fig. 8. Amount adsorbed against initial concentration for adsorption of Endosulfan pesticide using activated and unactivated boiler fly ash and maize cob

An increase in the initial pesticide concentration led to a corresponding increase in the adsorption capacity (q_e, $mg \cdot g^{-1}$). This behavior can be attributed to the greater availability of pesticide molecules at higher concentrations, which enhances the mass transfer driving force from the bulk solution to the adsorbent surface. The elevated concentration gradient reduces boundary layer resistance, thereby facilitating the diffusion of more molecules to occupy the available adsorption sites [27]. However, as q_e rises, the percent-removal falls at very high concentrations because the same number of sites must accommodate more molecules. This concentration-dependence is a common observation in adsorption studies and is routinely captured by isotherm models and explained by increased adsorbate–adsorbent driving force and site-saturation effects [28][29].

Activation of the adsorbent, improved the sorption capacity of the adsorbent, as can be seen that the activated adsorbents adsorbed more than the unactivated adsorbents. This could be as a result of two linked reasons: (1) physical/chemical activation increases specific surface area and accessible porosity (micropores and mesopores) so there are simply more sites for pore-filling and surface adsorption, and (2) activation alters surface chemistry-introducing or exposing oxygen-containing functional groups (–OH, –COOH, etc.) or changing surface polarity-which can strengthen interactions (hydrogen bonding, π–π, electrostatic or ligand-type interactions) with particular pesticide molecules. Together these textural and chemical changes normally lead to higher q_e and often faster uptake kinetics compared with the unactivated adsorbents [30].

Maize cob (MC) gave better sorption capacity than the boiler fly ash (BFA). This is consistent with many studies comparing biomass-derived activated carbons and unmodified industrial by-products. It has been reported that lignocellulosic precursors such as corn/maize cobs produce activated carbons with high surface areas, higher porosity and surface functional groups well suited for adsorbing organic pesticide molecules, whereas raw fly ash is predominantly inorganic (silica, alumina, unburnt carbon fractions) and usually requires chemical or thermal transformation to reach comparable affinity for organic pesticides [31]. Fly ash needs to be specifically functionalised or converted to a zeolite/carbon composite, otherwise, biomass-derived activated carbons commonly show superior sorption for many organic pesticides [10]. Similar results have been reported [32][33][29].

Mechanistically, for organochlorine and other hydrophobic pesticides, it has been reported that the dominant contributions are often (a) pore-filling of micropores/mesopores and (b) hydrophobic/van-der-Waals and π–π interactions with aromatic surface domains on activated carbon. For polar pesticides, electrostatic interactions and hydrogen bonding with surface oxygen groups become more important. Therefore, the better

performance of Act-MC likely reflects a combination of larger surface area/porosity and a surface chemistry that favours the adsorption of endosulfan pesticide [11][34][35].

3.3. Adsorption isotherm studies

Adsorption isotherms are crucial for understanding the mechanisms governing the uptake of pesticides such as endosulfan from aqueous solutions. The adsorption isotherm models used for this study are Langmuir [36] (Eq. 1), Freundlich [37] (Eq. 2), Dubunin-Radushkevich [38] (Eq. 3), Temkin (Eq. 4), Harkins and Jura (H-J) (Eq. 5), and Florry-Huggins (F-H) (Eq. 6), [39] isotherms. The linear form of these equations as shown below, were used to plot the equilibrium adsorption data.

Langmuir : $C_e/q_e = \frac{1}{(q_m K_L)} + C_e/q_m$ (1)

Freundlich : $\ln q_e = \ln K_F + \frac{1}{n}\ln C_e$ (2)

Dubunin-Radushkevich: $\ln q_e = \ln q_D - \beta\varepsilon 2$ (3)

Temkin : $q_e = B \ln A + B \ln C_e$ (4)

Harkins and Jura : $1/q_e 2 = \frac{B}{A} - \frac{1}{A}\log C_e$ (5)

Flurry-Huggins : $\log(\frac{\theta}{C}) = \log Ka + n \log (1 - \theta)$ (6)

In these models, q_e represents the amount adsorbed ($mg \cdot g^{-1}$), while C_e denotes the equilibrium concentration remaining in solution. K_L ($L \cdot g^{-1}$) is a constant associated with the adsorption–desorption energy, and q_m refers to the maximum adsorption capacity corresponding to complete saturation of the biomass surface. K_F and n are the Freundlich constants, whereas q_D is the Dubinin–Radushkevich (D–R) isotherm constant related to the extent of sorbate uptake by the sorbent surface. The Polanyi potential (ε) is defined as $\varepsilon = RT \ln(1 + 1/C_e)$, and β is related to the mean free energy of adsorption (E) per mole of sorbate as it migrates from the bulk solution to the biomass surface, expressed as $E\ (kJ \cdot mol^{-1}) = (2\beta)^{-1/2}$ [40,41]. The adsorption isotherm plots for the Langmuir, Freundlich, Dubinin–Radushkevich, Temkin, Harkins–Jura (H–J), and Flory–Huggins (F–H) models for endosulfan adsorption are presented in Figures 9–14.

Adsorption isotherm models are commonly employed to describe equilibrium sorption behavior [37][10][33][34][42]. The results indicate that different models adequately fitted the experimental sorption data, showing good agreement with the observed trends. The suitability of each model in describing equilibrium data is strongly influenced by the physicochemical properties of both the adsorbent surface and the adsorbate molecules. Among the widely applied models, the Langmuir and Freundlich isotherms are most frequently used to characterize pesticide adsorption, with numerous studies reporting the Freundlich model as providing the best fit to experimental sorption data [21][22][43].

The overall order of model fitness was determined as Freundlich > Langmuir > Temkin > Dubinin–Radushkevich (D–R) > Harkins–Jura (H–J) > Flory–Huggins (F–H). The Freundlich isotherm is particularly suitable for describing non-monolayer adsorption processes occurring on heterogeneous adsorbent surfaces [44][45]. It describes heterogeneous surface energies and multilayer adsorption, making it more applicable to natural and modified adsorbents [46][47]. Therefore, several studies have shown that the Freundlich isotherm often provides the best fit for endosulfan adsorption data, indicating heterogeneous surface adsorption and multilayer uptake, especially when agricultural wastes or biosorbents are used [29].

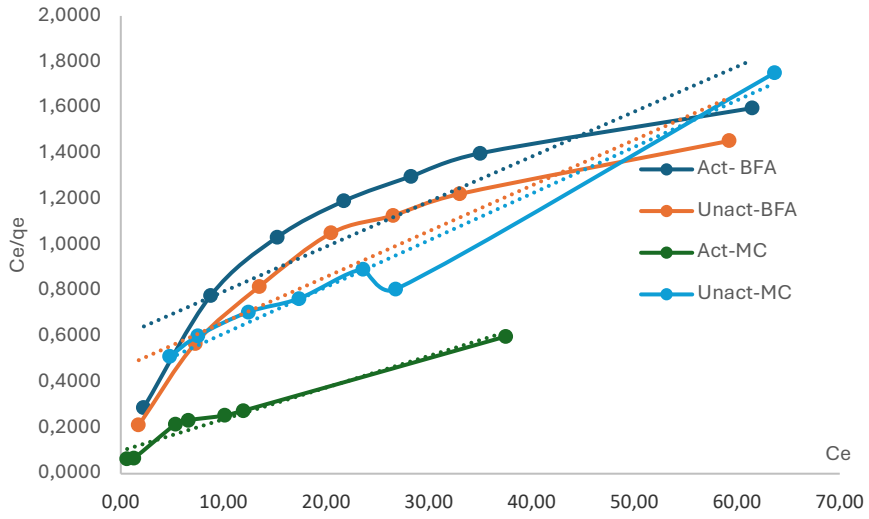

Fig. 9. Adsorption Isotherm plots for Langmuir adsorption of Endosulfan pesticide using activated (Act) and unactivated (Unact) boiler fly ash (BFA) and maize cob (MC)

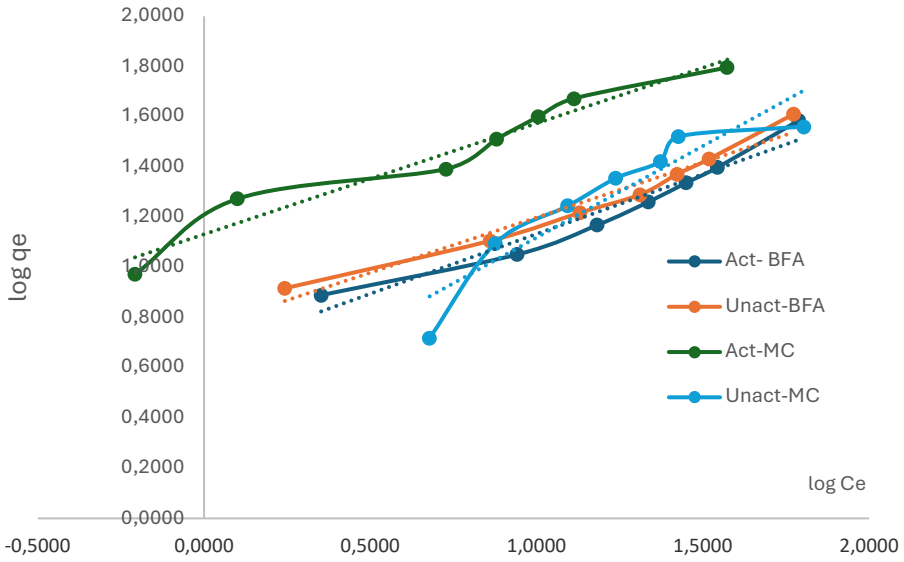

Fig. 10. Adsorption Isotherm plots for Freundlich adsorption of Endosulfan pesticide using activated (Act) and unactivated (Unact) boiler fly ash (BFA) and maize cob (MC)

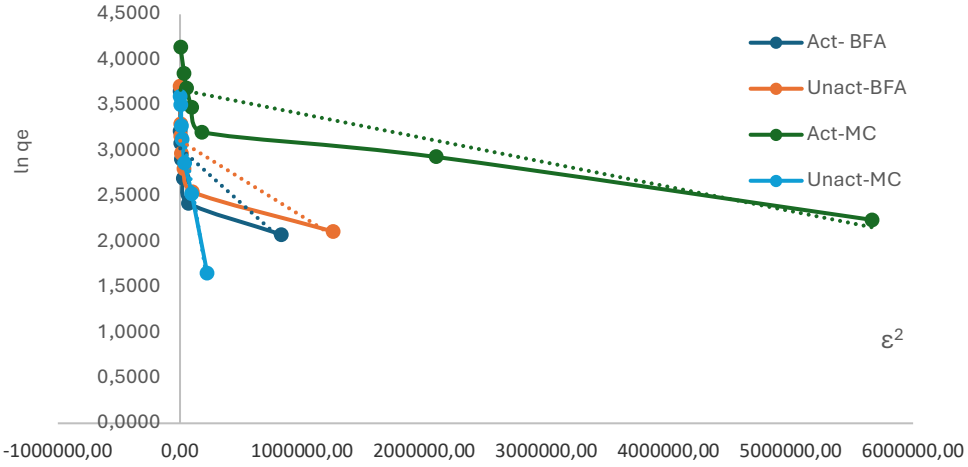

Fig. 11. Adsorption Isotherm plots for Dubinin-Radushkevich (D-R) adsorption of Endosulfan pesticide using activated (Act) and unactivated (Unact) boiler fly ash (BFA) and maize cob (MC)

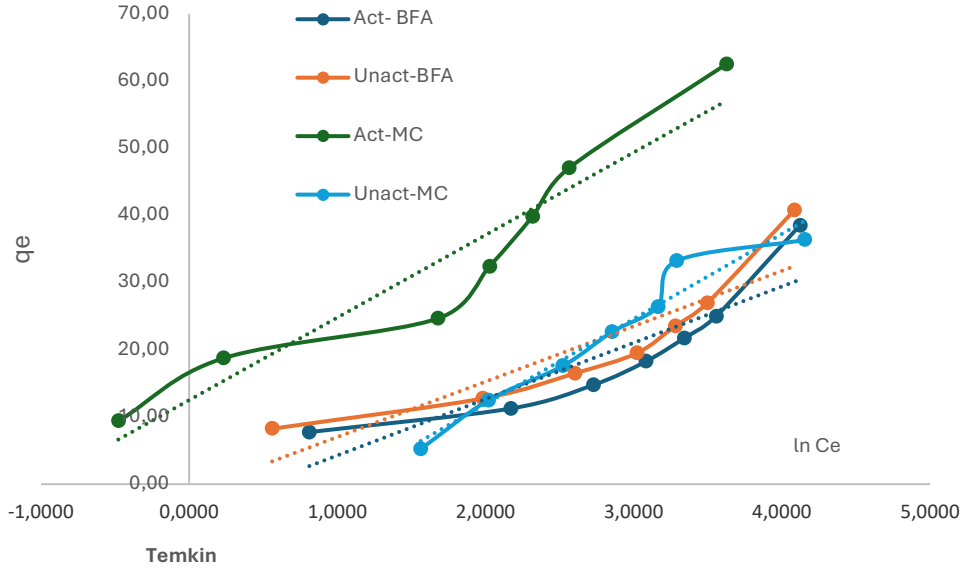

Fig. 12. Adsorption Isotherm plots for Temkin adsorption of Endosulfan pesticide using activated (Act) and unactivated (Unact) boiler fly ash (BFA) and maize cob (MC)

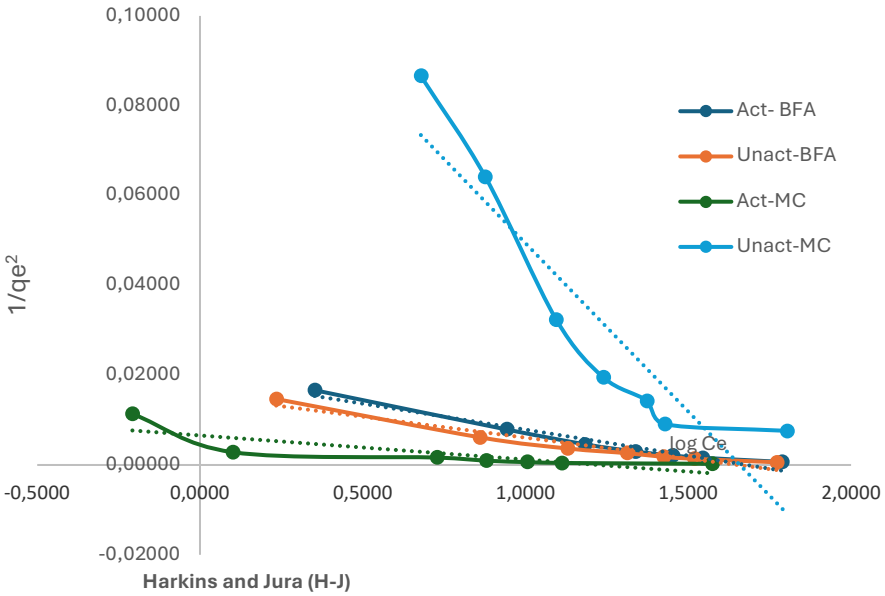

Fig. 13. Adsorption Isotherm plots for Harkins and Jura (H-J) adsorption of Endosulfan pesticide using activated (Act) and unactivated (Unact) boiler fly ash (BFA) and maize cob (MC)

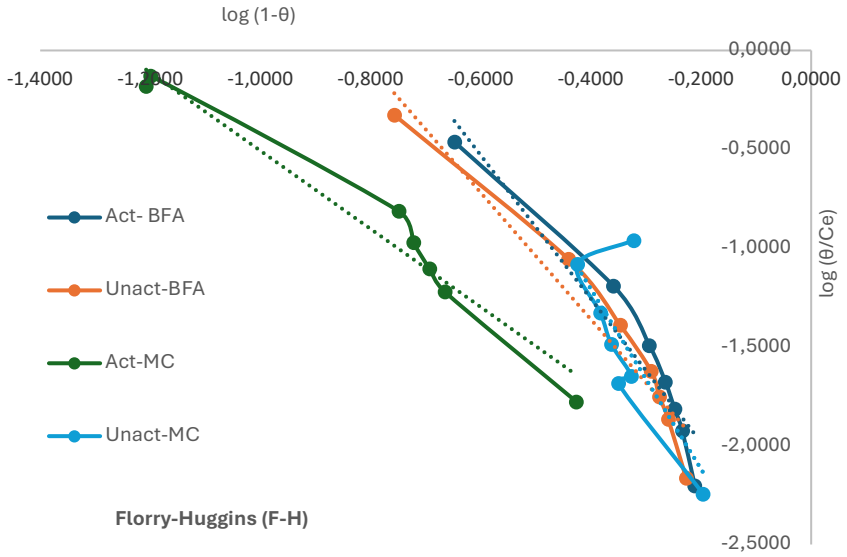

Fig. 14. Adsorption Isotherm plots for Flurry-Huggins (F-H) adsorption of Endosulfan pesticide using activated (Act) and unactivated (Unact) boiler fly ash (BFA) and maize cob (MC)

In some cases, the Langmuir isotherm has been found suitable, particularly when adsorption occurs via monolayer coverage on more uniform surfaces. It has been reported that endosulfan adsorption onto amine-modified magnetic diatomite fitted well with the Langmuir model, indicating finite adsorption sites and chemical affinity between endosulfan and surface groups [10]. The Langmuir separation factor (RL) in such studies typically indicated favorable adsorption ($0 < RL < 1$), reinforcing the applicability of the model. Other models, such as the Temkin isotherm, have also been applied to pesticide sorption. The Temkin model assumes adsorbate–adsorbent interactions and a uniform distribution of binding energies, while the D–R model helps in distinguishing between physical and chemical adsorption by estimating mean sorption energy [3]. These complementary models provide deeper insight into adsorption mechanisms beyond simple capacity estimation. Temkin and Dubinin–Radushkevich (D–R) isotherms were applied to describe endosulfan adsorption onto soil organic matter and was found out that adsorption was influenced by chemical interactions rather than purely

physical forces [6][48]. The D–R model further indicated that the mean sorption energy values were consistent with chemisorption processes. The coefficient of linear regression (R2) for all the isotherms and the isotherm constants were calculated and are shown in Table 2.

Table 2. Adsorption Isotherm constants for adsorption of Chlorpyrifos pesticide using activated and unactivated boiler fly ash and maize cob

S/N	Isotherm/Constants	Boiler fly ash (BFA)		Maize Cob (MC)	
		Unactivated BFA	Activated BFA	Unactivated MC	Activated MC
1.	Langmuir				
	q_m (mg/g)	50.251	51.020	49.020	72.464
	K_L (L/mg)	0.0432	0.3270	0.0501	0.1390
	R^2	0.7837	0.8247	0.9540	0.9727
2.	Freundlich				
	1/n	0.4763	0.4392	0.4424	0.7289
	K_F (mg/g)	5.7425	4.5341	2.4536	13.5363
	R^2	0.9469	0.9593	0.9523	0.8648
3.	D-R				
	β (mol^2/J^2)	1.0E-6	8.0E-7	3.0E-7	8.0E-6
	q_D (mg/g)	22.426	20.641	29.794	39.283
	R^2	0.5051	0.5546	0.7962	0.9431
	E (KJ/mol)	707.11	790.57	1291.00	250.00
4.	Temkin				
	A	0.8636	0.6074	0.3379	2.6892
	B	8.385	8.2470	12.294	12.647
	R^2	0.7898	0.8024	0.9198	0.9525
5.	H-J				
	A	107.527	86.207	13.333	185.185
	B	1.6560	1.681	1.657	1.222
	R^2	0.9552	0.9406	0.6784	0.8384
6.	Flurry-Huggins				
	Ka	2.275E-3	1.952E-3	9.358E-4	3.276E-3
	n	-3.206	-3.632	-4.554	-1.977
	R^2	0.9202	0.9392	0.9647	0.5785

Overall, the close fit of experimental data to Freundlich and related models highlights the complexity of adsorption processes, particularly for pesticides like endosulfan, where surface heterogeneity, pore structure, and adsorbate affinity significantly influence adsorption performance. The suitability of Freundlich isotherm in pesticide sorption studies suggests the presence of surface heterogeneity and varying adsorption energies. The Freundlich constant n, which indicates adsorption intensity, typically reflects a favourable adsorption process when values range between 1 and 10 [37][10][49]. From Table 3, it could be seen that 1/n ranged from 0.4392 for Act-BFA, 0.4424 for Unact-MC, 0.4763 for Unact-BFA to 0.7289 for Act-MC, which translates to n values of 2.28 for Act-BFA, 2.26 for Unact-MC, 2.10 for Unact-BFA to 1.37 for Act-MC. It could be seen that the n values are between 1 and 10. Several studies have demonstrated that activated agricultural residues exhibit this behaviour, confirming their effectiveness as low-cost and environmentally sustainable adsorbents [44][45][10][46][47].

Surface coverage is a critical parameter in adsorption studies, as it reflects the extent to which the adsorbent's surface is utilized for binding adsorbate molecules. The surface coverage was used to investigate the extent of coverage on the surface of the adsorbent by the adsorbate. It is given by equation (7).

$$\theta = (1 - C_e/C_o). \quad (7)$$

Where Ce is the equilibrium concentration and Co is the initial concentration. The plot of surface coverage (θ) versus initial concentration (Co) is shown in Figure 15.

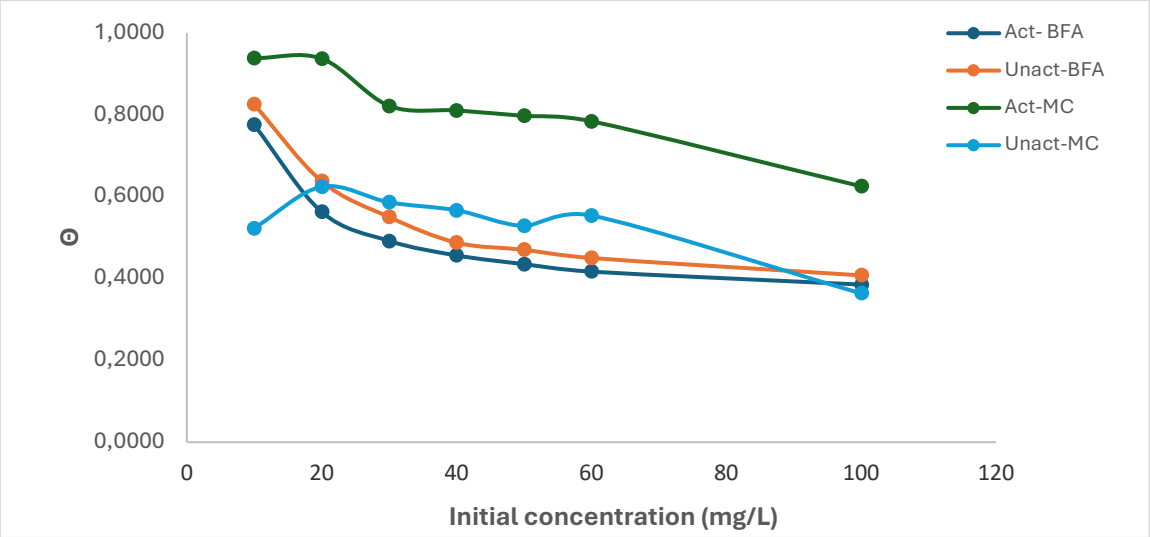

Fig. 15. Fractional Coverage against initial concentration for adsorption of Endosulfan pesticide using activated and unactivated boiler fly ash and maize cob

In this study, surface coverage was found to vary with initial concentration of the pesticide. At lower concentrations, the surface coverage was relatively higher. This suggests that at lower concentrations; the available active sites on the adsorbent are not saturated, thereby allowing a larger fraction of the surface to participate in the adsorption process. Conversely, as the initial concentration of adsorbate was increased, the surface coverage decreased. This decline may be attributed to competition among the excess adsorbate molecules for a finite number of surface binding sites. Once most of these sites are occupied, additional molecules remain unadsorbed in solution, thereby lowering the relative surface coverage [50]. This behaviour also reflects the principle of surface site saturation. Adsorption is inherently limited by the surface area and pore structure of the adsorbent; hence, beyond a certain concentration, further increases in adsorbate do not proportionally increase adsorption but instead decrease efficiency [51][52].

Comparative performance of the adsorbents revealed that activated maize cob (Act-MC) exhibited the highest surface coverage values, followed by unactivated maize cob (Unact-MC), unactivated boiler fly ash (Unact-BFA), and lastly activated boiler fly ash (Act-BFA). The superior performance of Act-MC may be linked to its enhanced porosity and higher surface area generated during activation, which increases the number of available adsorption sites and improves surface–adsorbate interactions. In contrast, Act-BFA showing the lowest values may be due to structural changes or possible pore collapse during activation, which reduced effective adsorption sites. The intermediate performance of Unact-MC and Unact-BFA suggests that the physicochemical characteristics of agricultural residues (such as maize cob) favour higher adsorption than industrial by-products like fly ash, unless carefully optimized. Generally, these observations highlight that both the initial adsorbate concentration and the physicochemical properties of the adsorbent jointly determine surface coverage and, by extension, adsorption efficiency [53][54].

3.4. Effect of contact time

The results from the effect of contact time are very important because it helps in the determination of the optimum contact time for the sorption process of Endosulfan pesticide. Contact time strongly influences the rate and extent of adsorption, as it determines how long the pesticide molecules interact with the active sites of the adsorbent. The effects of varying the contact time of the adsorption process are shown in 16 for adsorption of Endosulfan pesticide.

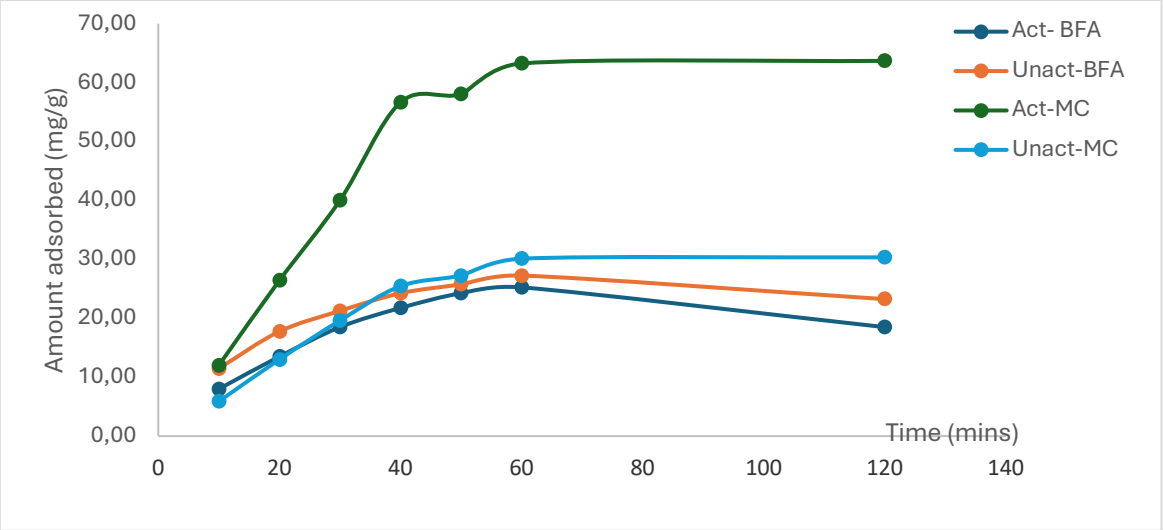

Fig. 16. Amount adsorbed against Time (mins) for adsorption of Endosulfan pesticide using activated and unactivated boiler fly ash and maize cob

The rate at which adsorption takes place has been reported as one of the very important factors for design of adsorption equipment. Also, kinetics has been reported as the controlling factor for sorbate residence time and reactor dimensions [55]. Generally, at the initial stages of contact, a rapid increase in adsorption is observed, which can be attributed to the availability of many vacant adsorption sites on the surface of the adsorbent. As time increases, these sites become progressively occupied, leading to a reduction in the adsorption rate until equilibrium is reached [56]. The results of this experiment agree with the above general observation as there was rapid adsorption at the initial time of 10 to 40 mins. As time was increased, the amount adsorbed also increased but not rapidly until it got to a maximum at 60 mins and then decreased. Thus, equilibrium was reached after about 60 mins.

At equilibrium, the amount of Endosulfan adsorbed remains nearly constant because the forward adsorption rate equals the backward desorption rate. For the design of effective water treatment systems, it is important to determine equilibrium or optimum contact time because it indicates the minimum time required for maximum pollutant removal without waste of energy or resources [57][27]. Beyond this point, extending the contact time does not significantly enhance adsorption but may even promote desorption due to competition between sorbate molecules and possible weakening of adsorbate–adsorbent interactions [58][59].

In pesticide adsorption studies, the optimum contact time depends on a lot of factors. For Endosulfan, which is hydrophobic and relatively persistent, sufficient contact time allows the molecules to diffuse into the internal pores of activated adsorbents, thereby enhancing adsorption efficiency [27][59]. Activated adsorbents such as boiler fly ash and maize cob derivatives often show shorter equilibrium times compared to unactivated forms due to improved porosity and surface area, which facilitates rapid adsorption dynamics [55][60]. Therefore, contact time experiments not only provide insights into adsorption kinetics but also guide in selecting the most suitable kinetic model, such as pseudo-first-order or pseudo-second order, to explain the mechanism of pesticide uptake. This knowledge is particularly vital for scaling up laboratory findings to field-scale applications in wastewater treatment and environmental remediation.

3.5. Sorption kinetics and intraparticle diffusion

Kinetic models are very important tools for understanding the mechanism of sorption and identifying the rate-limiting steps that control the process. Pseudo-first-order (PFO) and pseudo-second-order (PSO) kinetic models are amongst the most widely used models [59][60][61]. However, in many adsorption processes, particularly with hydrophobic and persistent pesticides such as Endosulfan, adsorption does not occur at the surface alone but also involves gradual penetration into the pores of the adsorbent. This behaviour is best described by the intra-particle diffusion, which evaluates whether diffusion into the internal pores of the adsorbent is the rate-limiting step [60].

The adsorption kinetics and intraparticle diffusion equations used for this study are pseudo-first order [21] (Eq. 8), pseudo-second order [22] (Eq. 9), Ritchie's second order [23] (Eq. 10), for adsorption kinetics; Penetrant transport equation (Eq. 11) Elovich equation (Eq. 12), and McKay and Poots (Eq. 13) equations [24][25][26], for intraparticle diffusion. The linear forms of these equations are as shown below:

Pseudo-first order $$log(q_e - q_t) = log\, q_e - \frac{K_1 t}{2.303} \quad (8)$$

Pseudo-second order $$\frac{t}{q_t} = \frac{1}{h_0} + \frac{t}{q_t} \quad \text{Where} \quad h_0 = K_2 q_e \quad (9)$$

Ritchie's second order equation $$\frac{1}{q_t} = \frac{1}{k q_0 t} + \frac{1}{q_e} \quad (10)$$

Penetrant transport equation $$log\, R = log\ \ Kid + a\, log\, t \quad (11)$$

Elovich equation $$q^t = \frac{1}{\beta} ln(\alpha\beta) + \frac{1}{\beta} ln\, t \quad (12)$$

McKay and Poots equation $$q^t = X_t + K^1 t^{0.5} \quad (13)$$

The plots for pseudo-first, pseudo-second, Ritchie's kinetic equations, Penetrant transport, Elovich and McKay and Poots are shown in Figure 17 - Figure 20, for Endosulfan adsorption.

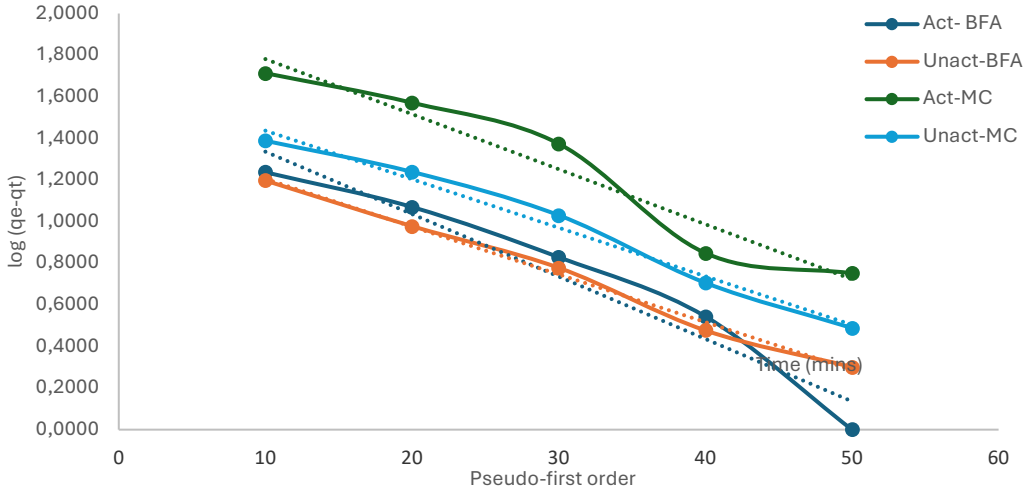

Fig. 17. Adsorption kinetics plots for Pseudo-first, Pseudo-second, Ritchie's kinetic equations for adsorption of Endosulfan pesticide using activated (Act) and unactivated (Unact) boiler fly ash (BFA) and maize cob (MC)

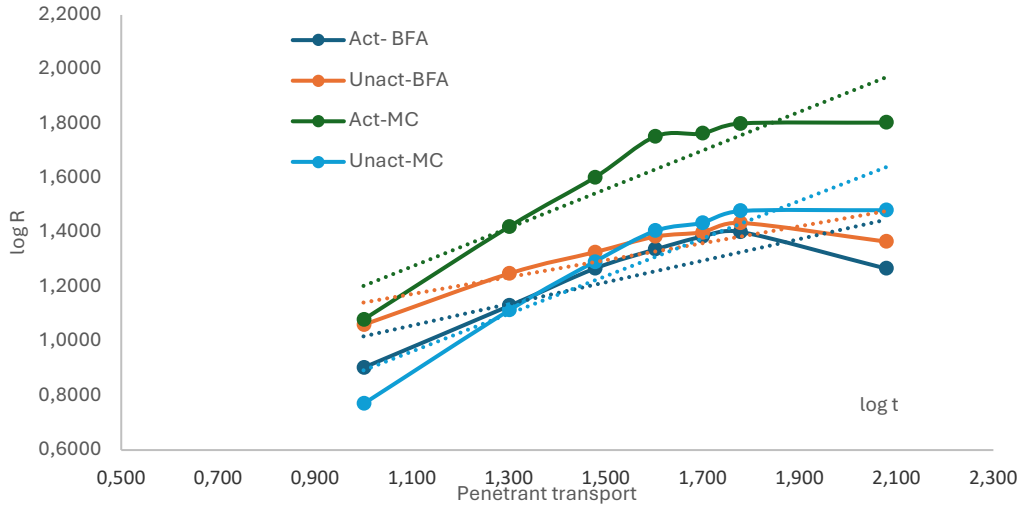

Fig. 18. Adsorption kinetics plots for Pseudo-first, Pseudo-second, Penetrant transport for adsorption of Endosulfan pesticide using activated (Act) and unactivated (Unact) boiler fly ash (BFA) and maize cob (MC)

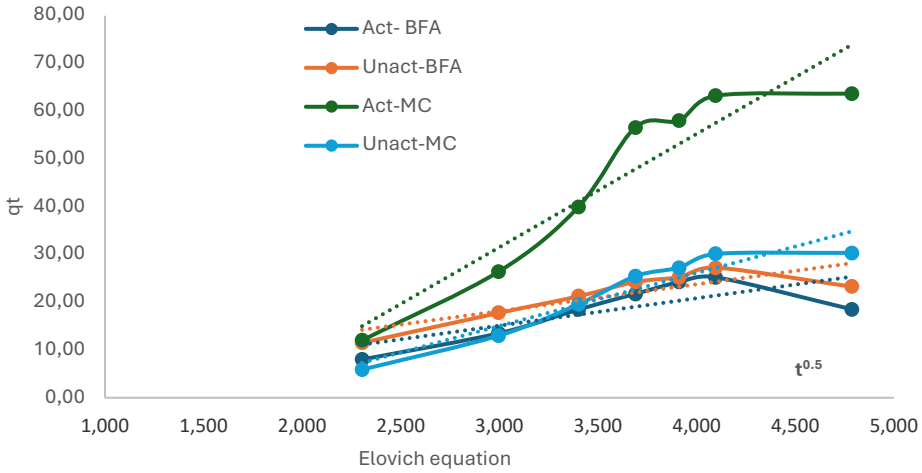

Fig. 19. Adsorption kinetics plots for Pseudo-first, Pseudo-second, Elovich for adsorption of Endosulfan pesticide using activated (Act) and unactivated (Unact) boiler fly ash (BFA) and maize cob (MC)

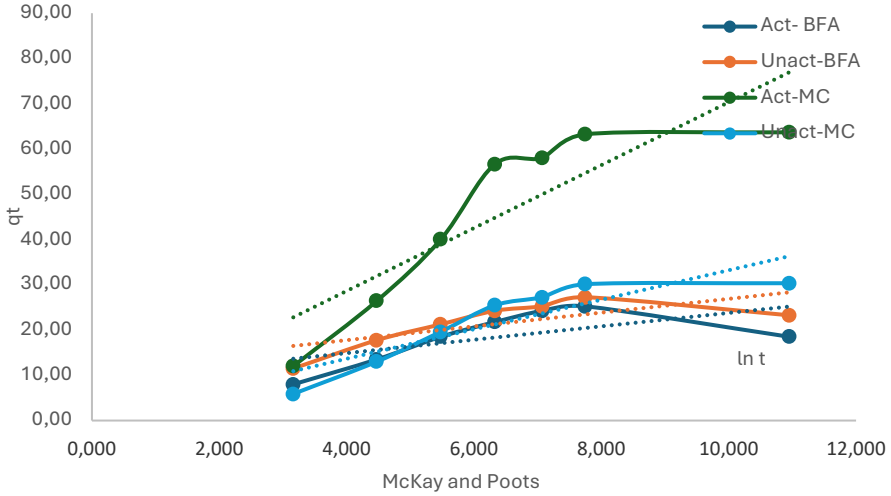

Fig. 20. Adsorption kinetics plots for Pseudo-first, Pseudo-second, McKay and Poots for adsorption of Endosulfan pesticide using activated (Act) and unactivated (Unact) boiler fly ash (BFA) and maize cob (MC)

Kinetic modelling describes the rate of adsorption and provides insights into rate controlling mechanisms. The PFO model assumes that the rate of adsorption is proportional to the number of unoccupied sites, reflecting physical adsorption processes dominated by external surface interactions and boundary layer effects. If the data for Endosulfan adsorption fit the PFO model, it indicates that the uptake is controlled largely by surface diffusion and weaker Van der Waals forces [58][59]. On the other hand, the PSOis based on the assumption that chemisorption governs the adsorption rate. This involves stronger interactions, such as hydrogen bonding, π–π electron donor–acceptor interactions, or covalent bonding between the pesticide molecules and functional groups present on the adsorbent surface. Many studies have shown that pesticide adsorption on modified agro-wastes and industrial by-products tends to align more closely with the PSO model, reflecting enhanced surface reactivity and intra-particle interactions [50][60][61]. The results of this study showed that the PSO kinetic model gave a better fit to the adsorption kinetic data.

Intraparticle diffusion models further reveal the contribution of pore diffusion and boundary layer resistance to overall adsorption rates. When experimental data are plotted as the amount adsorbed (qt) against the square root of time (t0.5), a linear relationship suggests intra-particle diffusion. If the line passes through the origin, then intra-particle diffusion is the sole rate-limiting step. However, if the line does not pass through the origin, it indicates that other processes such as film diffusion or surface adsorption are also contributing to the overall mechanism [57][27]. In practice, Endosulfan adsorption often exhibits a multi-linear plot in the intra-particle diffusion model, suggesting two or more stages: an initial rapid uptake due to surface adsorption, followed by a slower phase governed by intra-particle diffusion. Activated adsorbents typically show enhanced

intra-particle diffusion due to increased pore volume and surface functionalization, whereas unactivated adsorbents may exhibit limited pore accessibility, making surface adsorption the dominant mechanism [50][60][61]. The penetrant transport model gave a better fit to the intra-particle diffusion data for the pesticide adsorption kinetic data.

In addition, the application of these models allows for the determination of adsorption rate constants, which are critical parameters in designing batch and continuous water treatment systems. The suitability of one model over the other not only reflects the mechanism of adsorption but also indicates the efficiency of adsorbent modification in improving pesticide removal from aqueous solutions. The constants for the kinetic and intraparticle diffusion studies are shown in Table 4for Endosulfan adsorption. It could be seen that for penetrant transport, penetrant a < 1, while penetrant Kid> 1. Penetrant a-values represents the likelihood and degree of strive; where, a >1 indicates the presence of high strive, a < 1 depicts moderate strive while for a <1, the adsorption process may not be due to adsorbate core strive [24]. Again, penetrate Kid value of an adsorption system is usually less than 1 for an interaction between adsorbent and adsorbate which is dominated by ion-exchange [24]. From the results of this study, a-values are <1 and Kid>1. This means that there is an indication that dipole induced dipole interactions are dominant. This also supports van der Waals forces of attraction.

Therefore, combining PFO, PSO, and IPD kinetic analyses provides a comprehensive understanding of Endosulfan sorption behavior, distinguishing between physisorption and chemisorption and predicting long-term adsorption performance, While the PSO model often gives the best overall fit, the intra-particle diffusion model adds valuable insights into the diffusion-controlled steps, which is particularly important for optimizing adsorbent selection for scaling up batch adsorption experiments to continuous systems in environmental remediation.

Table 3. Adsorption kinetics and intraparticle diffusion constants for adsorption of Chlorpyrifos pesticide using activated and unactivated boiler fly ash and maize cob

S/N	Isotherm/Constants	Boiler fly ash (BFA)		Maize Cob (MC)	
		Unactivated BFA	Activated BFA	Unactivated MC	Activated MC
1.	Pseudo-First order				
	q_e (mg/g)	27.17	43.25	46.78	111.07
	K_1	0.0527	0.0691	0.0537	0.0610
	R^2	0.9476	0.9946	0.9426	0.9847
2.	Pseudo-second				
	q_e (mg/g)	25.51	20.83	44.84	96.15
	K_2	0.0075	0.0127	0.0005	0.0003
	h_0	4.859	5.5190	1.002	2.1180
	R^2	0.9212	0.97.21	0.8312	0.8783
3.	Ritchie's second order				
	q_e (mg/g)	33.11	34.97	163.93	454.55
	K	0.0551	0.0310	0.0039	0.0028
	R^2	0.9156	0.9465	0.9731	0.9735
4.	Penetrant				
	K_{id}	6.773	4.174	1.587	3.108
	a	0.3977	0.3117	0.7113	0.6926
	R^2	0.6242	0.7160	0.8450	0.8531
5.	Elovich				
	β	0.1780	0.1744	0.0902	0.0421
	α	5.8735	-6.5195	-14.4048	-27.7340
	R^2	0.5635	0.7068	0.8878	0.9091
6	McKay and Poots				
	X_t	8.975	11.678	0.8272	0.6153
	K^1	1.4804	1.5208	6.9509	3.2600
	R^2	0.3715	0.5119	0.7530	0.7770

In other to study the trend of the attainment to equilibrium, the fractional attainment to equilibrium 'α' for adsorption of Endosulfan pesticide using activated and unactivated boiler fly ash and maize cob was evaluated using Eq. 20. [24]. The plot is shown in Figure 21.

$$\alpha = [X]_{eq}/[X]_t \quad (20)$$

Where $[X]_{eq}$ and $[X]_t$ is the concentration of the specie at equilibrium at time t respectively.

The mechanism of diffusion which precedes adsorption has been broadly divided into intra-particle diffusion and film diffusion mechanism. As diffusion precedes adsorption, the fractional attainment to equilibrium (FATE) is the rate of mass transfer from the liquid phase to the solid adsorbent phase (Abia and Didi, 2007).

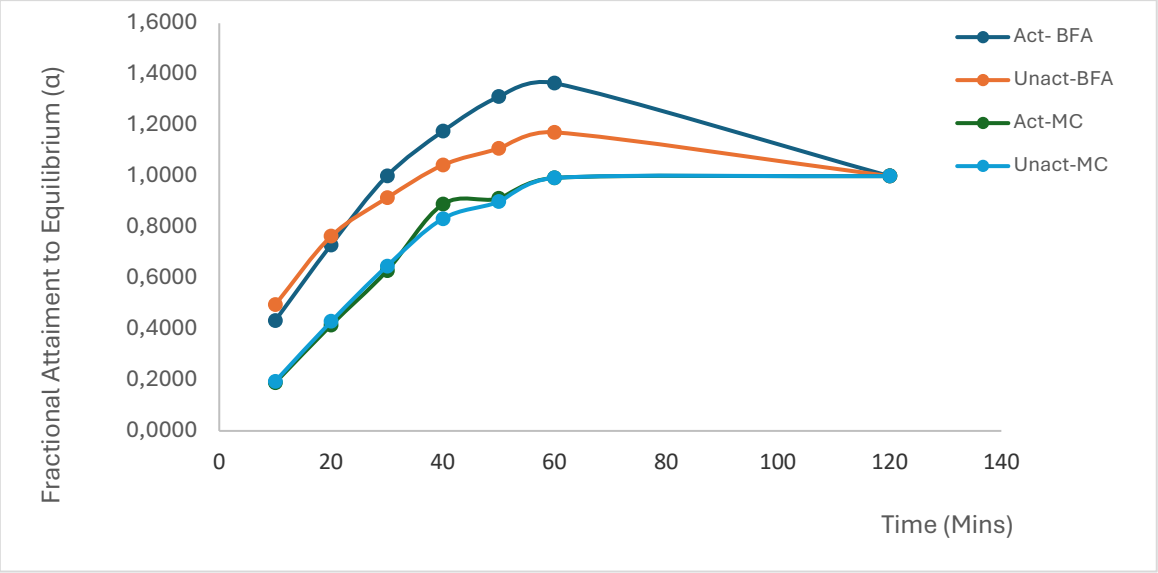

Fig. 21. Fractional Attainment to Equilibrium for adsorption of Endosulfan pesticide using activated and unactivated boiler fly ash and maize cob

In this study, adsorption of endosulfan was very rapid during the first 0–60 minutes of contact time. This fast uptake at the initial stage is attributed to the availability of many vacant and easily accessible active sites on the surface of the adsorbent. At this stage, pesticide molecules encounter little resistance in diffusing to the adsorption sites, and the process is largely governed by external surface adsorption [56]. After the initial period, the adsorption rate decreased slightly, indicating that many of the readily available active sites had already been occupied. As adsorption progressed, repulsive forces between the adsorbed pesticide molecules and those still in solution, as well as intraparticle diffusion limitations, slowed the process [58][59]. At this point, equilibrium was reached as discussed earlier and this has been reported [62][63][57][27].

3.6. Modelling the Equilibrium Sorption Data

Isotherm modelling not only validates experimental observations but also informs the design of adsorption systems for water treatment applications. Also, the adsorption isotherm modelling of endosulfan reveals that the Freundlich model is most often reported as the best fit, due to the heterogeneous nature of most adsorbents. However, depending on surface characteristics, the Langmuir, Temkin, and D–R models provide additional mechanistic insights. Such findings highlight the complexity of endosulfan adsorption and the necessity of applying multiple isotherm models to obtain a holistic understanding of the process.

The equilibrium adsorption isotherm constants obtained from the linear equations (Eq.1 - Eq.6), shown in Table 2 were used together with the predictive models (Eq.21 - Eq.26) derived from Eq. 1 to Eq. 6 for the respective isotherms to predict the values of amount adsorbed (qe) for each value of equilibrium concentration (Ce) as seen by the linear forms of the isotherms. These values of qe for the isotherms were compared to the experimental value to confirm the isotherm model that best fits the equilibrium experimental results.

Langmuir: $$q_e = \frac{q_m K_L C_e}{(1+K_L C_e)} \quad (21)$$

Freundlich: $$q_e = K_F C_{e\frac{1}{n}} \quad (22)$$

Dubunin-Radushkevich: $$q_e = qD\exp\left(-\beta\left[RT\ln\left(1+\frac{1}{C_e}\right)\right]^2\right) \quad (23)$$

Temkin: $$q_e = K_T C_e{}^b \quad (24)$$

Harkins and Jura: $$q_e = \left(\frac{A}{B\log C_e}\right) \quad (25)$$

Flurry-Huggins: $$q_e = C_o{}^{1-n}\, C_e{}^{1+n}\, K_a \quad (26)$$

The plots of these predictive models are given in Figure 22 – Figure 25 for adsorption of Endosulfan pesticide using Act-BFA, Unact-BFA, Act-MC and Unact-MC. The results from these isotherm models were compared to the experimental values of the adsorption process to help give an insight to the goodness of fit of the isotherms and help identify the isotherm of best fit.

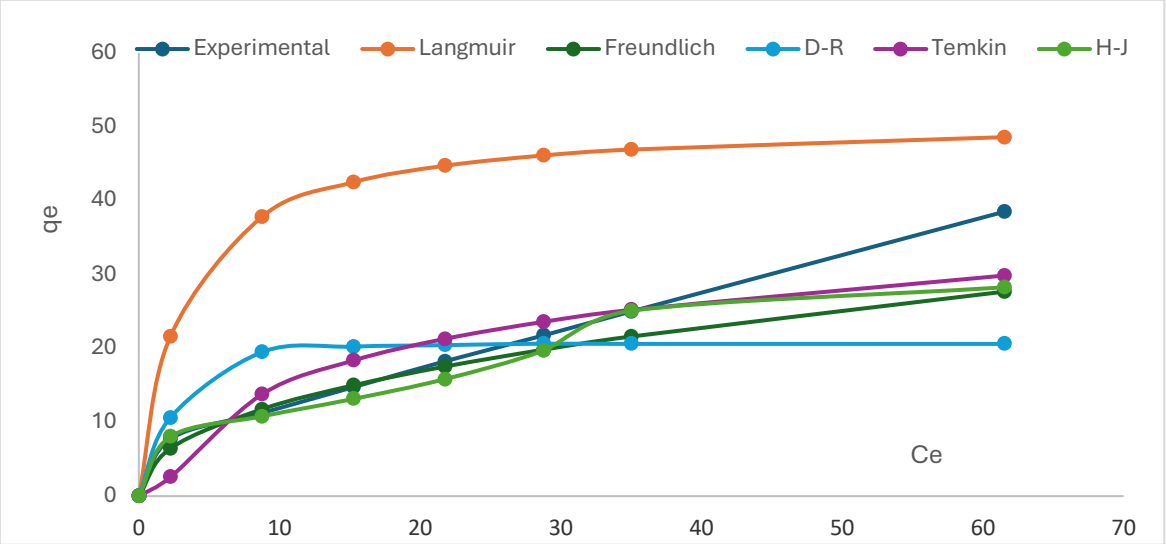

Fig. 21. Isotherm models for adsorption of endosulfan pesticide using Act-BFA

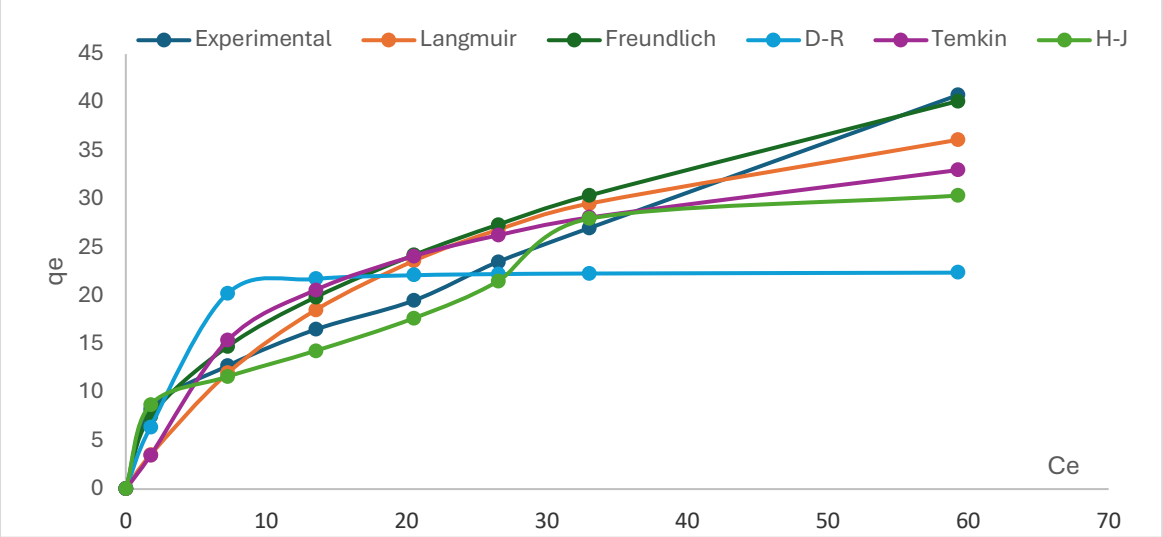

Fig. 22. Isotherm models for adsorption of endosulfan pesticide using Unact-BFA

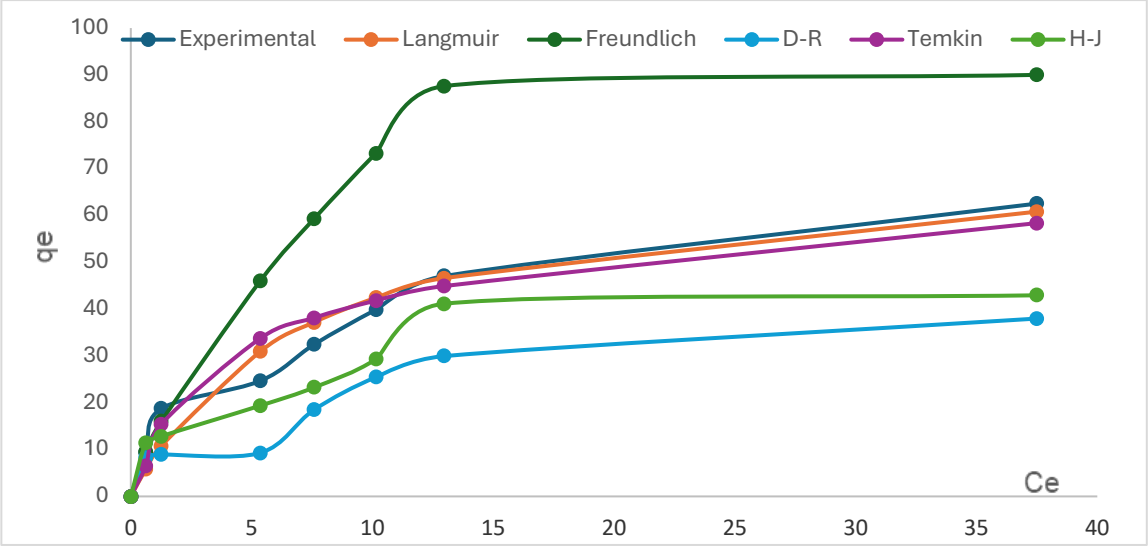

Fig. 23. Isotherm models for adsorption of endosulfan pesticide using Act-MC

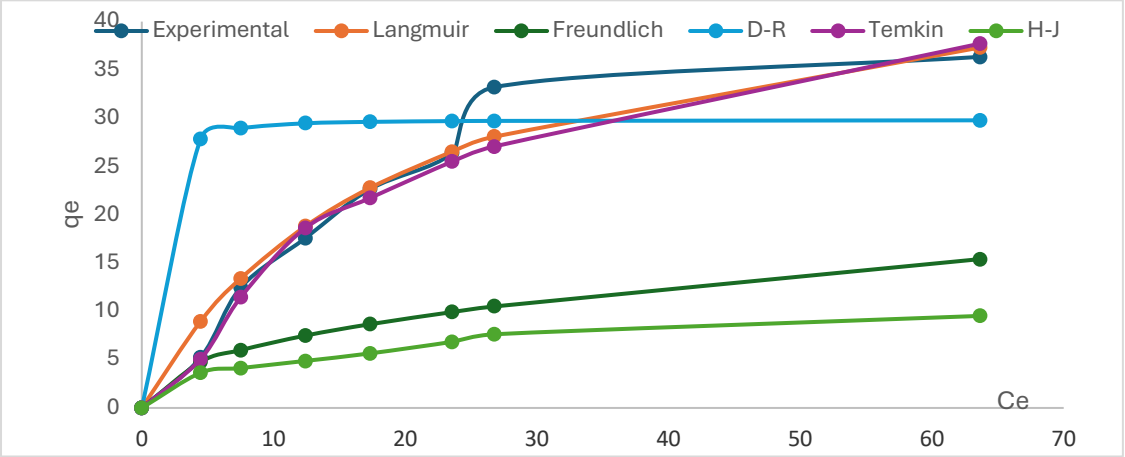

Fig. 24. Isotherm models for adsorption of endosulfan pesticide using Unact-MC

The comparison of the calculated equilibrium adsorption capacities (qe) from isotherm models with the experimental values is critical in validating the suitability of the predictive models. When the theoretical qevalues closely match the experimental data, it indicates that the chosen model adequately describes the adsorption mechanism and equilibrium behaviour under the studied conditions. Predictive isotherm models, for Langmuir, Freundlich, Temkin, Dubinin–Radushkevich (D-R) and Harkins-Jura (H-J), provide insights into surface heterogeneity, adsorption intensity, and the nature of the interactions between adsorbate and adsorbent. The conditions for applicationof these models have earlier been discussed.

Therefore, generally the isotherm model that produces qevalues closest to the experimental data is considered the most reliable for predicting adsorption performance. This validation not only improves mechanistic understanding but also supports the scale-up and practical design of adsorption-based water treatment systems for pesticide removal. From the results of the models applied to this experiment, it was found out that the Freundlich isotherm gave a better fit to the sorption experimental data for adsorption of endosulfan using Act-BFA, Unact-BFA, Act-MC and Unact-MC. The trend of fitness of the isotherm was confirmed to be Freundlich > Langmuir > Temkin > Dubinin-Radushkevich (D-R) > Harkins-Jura (H-J) > Flurry-Huggins (F-H), as was given earlier.

4. CONCLUSION

The findings of this research clearly establish that both activated and unactivated boiler fly ash and maize cob possess significant potential as cost-effective and sustainable adsorbents for the removal of Endosulfan

pesticide from aqueous solutions. The application of mathematical modelling provided a deeper understanding of the adsorption mechanisms, equilibrium relationships, and predictive capabilities of the process. The models employed were consistent with the experimental results, thereby confirming their suitability for describing the adsorption behaviour of Endosulfan under the studied conditions. Activation of the adsorbents was shown to improve surface characteristics such as porosity and cation exchange capacity, which in turn enhanced adsorption efficiency compared to their unactivated counterparts. This underscores the role of chemical activation in optimizing the performance of agricultural by-products for water treatment. Furthermore, the ability of maize cob and boiler fly ash to act as alternative adsorbents demonstrates the importance of converting agricultural residues and industrial by-products into value-added resources for environmental management. The successful modelling of adsorption data not only validates the experimental observations but also provides a useful tool for predicting performance under different operational conditions, which is vital for large-scale applications. These results contribute to the growing body of knowledge supporting the use of bio-waste and industrial residues in the development of eco-friendly and low-cost treatment technologies. Therefore, this study reinforces the feasibility of employing activated and unactivated boiler fly ash and maize cob in pesticide remediation, thereby promoting sustainable approaches to water purification and pollution control.

Acknowledgments

The authors are very delighted to extend their warmest regards to the Tertiary Education Trust Fund (TETFUND) for the research grant to carry out this research through IBRF grant cycle 2024 with reference number TETFund/IBR/ABSU/2024/026to Professor B.O. Osu.

REFERENCES

[1] Menezes, R.G., Qadir, T.F., Moin, A., Fatima, H., Hussain, S.A., Madadin, M., Pasha, S.B., Al Rubaish, F.A. & Senthilkumaran S. (2017). Endosulfan poisoning: An overview. Journal of forensic and legal medicine 51, 27-33.

[2] Berdowska A, Bandurska K. (2025). Health Hazards Associated with Exposure to Endosulfan: A Mini-Review. Toxics.13(6), 455. doi: 10.3390/toxics13060455.

[3] Rauf, N., Tahir, S.S., Kang, J-H. & Chang, Y-S. (2012). Equilibrium, thermodynamics and kinetics studies for the removal of alpha and beta endosulfan by adsorption onto bentonite clay, Chemical Engineering Journal, 192,369-376, doi.org/10.1016/j.cej.2012.03.047.

[4] Sishu, F. K., Tilahun, S. A., Schmitter, P., Assefa, G., & Steenhuis, T. S. (2022). Pesticide Contamination of Surface and Groundwater in an Ethiopian Highlands' Watershed. Water, 14(21), 3446. https://doi.org/10.3390/w14213446.

[5] Mathanakeerthi, S., Sadheesh, S., Nandha Kumar, M., Gowtham, S.& Manoj Kumar, V. (2021).Adsorption of endosulfan from aqueous solution using graphene clay matrix (GCM), Materialstoday Proceedings, 45(6), 5665-5671.

[6] Vaikosen, E.N., Worlu, R.C., Bunu, S.J., Dode, E & Doctor, M. (2023). Liquid-Liquid Separation and Determination of Betamethasone, Clotrimazole and Neomycin in Topical Cream By UV-Visible Spectrophotometry, Int. J. in Pharm. Sci., 1(4), 170-179.

[7] Eun, H., Choi, G., Choi, D-S. & Hong, S-M. (2021). Performance Evaluation for Endosulfan Removal by Carbon-based Adsorbents Korean J. Pestic. Sci. 25(2), 111-118.

[8] Nader M. S. & Elkhatib. E.A. (2018). Kinetics and Thermodynamics of β-1Endosulfan Pesticide Adsorption in Jordan Valley Soils. Global Journal of Science Frontier Research, 18(B1), 1–10.

[9] Wang, Y., Wang, S. L., Xie, T. & Cao, J. (2020) Activated carbon derived from waste tangerine seed for the high-performance adsorption of carbamate pesticides from water and plant, Bioresource Technology, 316, 123929.

[10] Alacabey İ. (2022). Endosulfan Elimination Using Amine-Modified Magnetic Diatomite as an Adsorbent. Front. Chem. 10, 907302. doi: 10.3389/fchem.2022.907302.

[11] Vaikosen, E. N., Davidson, C.M. Olu-Owolabi, B. I., Gibson, L. T., Agunbiade, F. O., Kashimawo, A.J., Adebowale, K. O. (2022) Kinetic and isotherm studies on the adsorption–desorption of technical-grade endosulfan in loamy soils under Theobroma cacao L cultivation, Southwestern Nigeria.Environmental Science: Advances, 2(2), 257-277. (https://doi.org/10.1039/d2va00090c).

[12] Iizuka, T., Yahata, M. & Shimizu, A. (2013). Potential Mechanism Involved in Removal of Hydrophobic Pesticides from Vegetables by Hydrostatic Pressure. J. Food Eng. 119, 1–6.

[13] Rasolonjatovo, M. A., Cemek, M., Cengiz, M. F., Ortaç, D., Konuk, H. B., Karaman, E., et al. (2017). Reduction of Methomyl and Acetamiprid Residues from Tomatoes after Various Household Washing Solutions. Int. J. food Prop. 20, 2748–2759.

[14] Fathallah, T.Z., Hussein, T.Kh., Naeem, Y.A., Resan Abdulamer, R., Kyhoiesh, H.A.K. & Harfouch, M.A. (2024). Removal of Pesticides from Aqueous Solutions Using Recycled Waste Hydrogel as a Low-Cost Adsorbent, Asian Journal of Green Chemistry 8, 549-559.

[15] Mihajlović, M.T., Lazarević, S.S., Janković-Častvan, I.M., Kovač, J., Jokić, B.M., Janaćković, D.T. &Rada D. Petrović, R.D. (2015). Kinetics, thermodynamics, and structural investigations on the removal of Pb2+, Cd2+, and Zn2+ from multicomponent solutions onto natural and Fe (III)-modified zeolites. Clean Techn Environ Policy 17, 407–419.

[16] Sen T.K. (2023). Agricultural Solid Wastes Based Adsorbent Materials in the Remediation of Heavy Metal Ions from Water and Wastewater by Adsorption: A Review. Molecules. 28(14), 5575. doi: 10.3390/molecules28145575.

[17] Bayuo, J., Rwiza, M.J., Oyelude, E.O., Mtei, K.M. & Choi, J.W. (2025). Green adsorbent from maize biomass for mercury capture: Insights from sorption modeling and thermodynamic analysis. Applied Water Science, 15, 185-200. doi.org/10.1007/s13201-025-02546-7.

[18] Igwe, J.C., Okoronkwo, N.E & Okoli, E.A (2014). Adsorption studies of Chlorpyrifos and Endosulfan Pesticides from aqueous solution using coconut fibre. J. Chem. Soc. Nigeria. 39(2), 44-50.

[19] Ewis, D., Ba-Abbad, M.M., Benamor, A. & El-Naas, M.H. (2022). Adsorption of organic water pollutants by clays and clay minerals composites: A comprehensive review Applied Clay Science, 229, 106686. doi.org/10.1016/j.clay.2022.106686.

[20] Ungureanu, E. L., Mocanu, A. L., Stroe, C. A., Panciu, C. M., Berca, L., Sionel, R. M., & Mustatea, G. (2023). Agricultural By-products Used as Low-Cost Adsorbents for Removal of Potentially Toxic Elements from Wastewater: A Comprehensive Review. Sustainability, 15(7), 5999- 6033. doi.org/10.3390/su15075999.

[21] Kowanga, K.D., Gatebe, E., Mauti, G.O. & Mauti, E.M. (2016). Kinetic, sorption isotherms, pseudo-first-order model and pseudo-second-order model studies of Cu(II) and Pb(II) using defatted Moringa oleifera seed powder, The Journal of Phytopharmacology 5(2), 71-78.

[22] Li, J., Dong, X., Liu, X., Xu, X., Duan, W., Park, J., Gao, L. & Lu, Y. (2022). Comparative Study on the Adsorption Characteristics of Heavy Metal Ions by Activated Carbon and Selected Natural Adsorbents. Sustainability, 14, 15579-15596.

[23] Al-Sou'od, K. (2012). Kinetics of the adsorption of hexavalent Chromium from aqueous solutions on low-cost material. African Journal of Pure and Applied Chemistry 6(14), 190-197.

[24] Abia, A.A. & Didi, O. (2007). Transfer zone behaviour of As (III), Co (II) and Mn (II) ions on sulphur-hydryl infused cellulose surface. Afr. J. Biotechnology 6(3), 285-289.

[25] Malkoc E.&Nuhoglu Y. (2007). Determination of kinetic and equilibrium parameters of the batch adsorption of Cr (VI) onto waste acorn of Quercus ithaburensis. Chemical Engineering and Processing 46, 1020-1029.

[26] Özacar M, I.A. Sengil and H. Turkmenler (2008). Equilibrium and kinetic data and adsorption mechanism for adsorption of lead onto Valonia tannin resin. ChemicalEngineering Journal 143 (1-3), 32-42.

[27] Gholami M, Mosakhani Z, Barazandeh A, Karyab H. (2022). Adsorption of organophosphorus malathion pesticide from aqueous solutions using nano-polypropylene-titanium dioxide composite: Equilibrium, kinetics and Optimization studies. J Environ Health Sci Eng. 21(1), 35-45. doi: 10.1007/s40201-022-00826-x.

[28] Andrunik M, Skalny M, Gajewska M, Marzec M, Bajda T. (2023). Comparison of pesticide adsorption efficiencies of zeolites and zeolite-carbon composites and their regeneration possibilities. Heliyon. 9(10), e20572. doi: 10.1016/j.heliyon.2023.e20572.

[29] Luttah, I., Onunga, D.O., Shikuku, V.O., Otieno, B. & Kowenje, C.O. (2023), Removal of endosulfan from water by municipal waste incineration fly ash based geopolymers: Adsorption kinetics, isotherms, and thermodynamics. Front. Environ. Chem. 4, 1164372 - 1164385.

[30] Karume, I., Bbumba, S., Tewolde, S. Mukasa Is'harq Z. T. & Ntale, M. (2023). Impact of carbonization conditions and adsorbate nature on the performance of activated carbon in water treatment. BMC Chemistry17, 162 -174. https://doi.org/10.1186/s13065-023-01091-1.

[31] He X, Chen X, Wang X & Jiang L. (2023). Optimization of activated carbon production from corn cob using response surface methodology. Front. Environ. Sci. 11, 1105408-1105419. doi: 10.3389/fenvs.2023.1105408.

[32] Lazarotto, J.S.; da Boit Martinello, K.; Georgin, J.; Franco, D.S.P.; Netto, M.S.; Piccilli, D.G.A.; Silva, L.F.O.; Lima, E.C.; Dotto, G.L. (2021). Preparation of Activated Carbon from the Residues of the Mushroom (Agaricus bisporus) Production Chain for the Adsorption of the 2,4-Dichlorophenoxyacetic Herbicide. J. Environ. Chem. Eng.,9, 106843.

[33] Murtala, M.A., Aminu, K.R., Sanusi K.A. & Abdurrahman, B. (2022). Adsorption of Pesticides from Aqueous Solution using Kinkeliba (Combretum micranthum G.) Derived Activated Carbon International Journal of Sciences: Basic and Applied Research (IJSBAR) 63(2), 308-319.

[34] Harabi, S., Guiza, S., Alvarez-Montero, A., Gomez-Aviles, A., Bagane, M., Belver, C. & Bedia, J. (2024). Adsorption of Pesticides on Activated Carbons from Peach Stones. Processes, 12, 238 -255.

[35] Magdy A, Mostafa M.R, Moustafa S.A, Mohamed G.G, Fouad O.A. (2024). Kinetics and adsorption isotherms studies for the effective removal of Evans blue dye from an aqueous solution utilizing forsterite nanoparticles. Sci Rep. 14(1), 24392. doi: 10.1038/s41598-024-73697-x.

[36] Guo, X. & Wang, J. (2019). Comparison of linearization methods for modeling the Langmuir adsorption isotherm, Journal of Molecular Liquids, 296, 111850.

[37] Al-Ghouti M.A. & Da'ana D.A. (2020). Guidelines for the use and interpretation of adsorption isotherm models: A review, Journal of Hazardous Materials, 393, 122383.

[38] Wang, J. & Guo, X. (2020). Adsorption isotherm models: Classification, Physical meaning, Application and solving methods, Chemosphere, 258, 127279.

[39] Hu, Q., Lan, R., He, L., Liu, H. & Pei, X. (2023). A critical review of adsorption isotherm models for aqueous contaminants: Curve characteristics, site energy distribution and common controversies, Journal of Environmental Management, 329, 117104.
[40] Igwe, J.C. & Abia A.A (2005). Sorption Kinetics and Intraparticulate diffusivities of Cd, Pb and Zn ions on maize cob. African Journal of Biotechnology, 4(6), 509-512.
[41] Igwe, J.C., Nwadire, F.C. & Abia A.A (2012). Kinetics and Equilibrium Isotherms of Pesticides adsorption onto Boiler fly ash Terrestrial and Aquatic Environmental Toxicology, 6(1), 23-29.
[42] Sunartaty, R., Muslim, A. & Sri Aprilia1, M. (2024).NaOH-Activated Tofu Waste Adsorbent for Pb(II) and Cu(II) Adsorption: Kinetic and Isotherm studies. Journal of Environmental Research, Engineering and Management 80(2), 24-38. 10.5755/j01.erem.80.2.35898.
[43] Adesanmi BO, Mantripragada S, Ayivi RD, Tukur P, Obare SO, Wei J. (2024). Adsorptive removal of organophosphate pesticides from aqueous solution using electrospun carbon nanofibers. Front Chem. 12, 1454367. doi: 10.3389/fchem.2024.1454367.
[44] Afroze, S., Sen, T.K. & Ang, H.M. (2016). Adsorption removal of zinc (II) from aqueous phase by raw and base modified Eucalyptus sheathiana bark: Kinetics, mechanism and equilibrium study. Process Saf. Environ. Prot., 102, 336–352.
[45] An, F.-Q., Wu, R.-Y., Li, M., Hu, T.-P., Gao, J.-F. & Yuan, Z.-G. (2017). Adsorption of heavy metal ions by iminodiacetic acid functionalized D301 resin: Kinetics, isotherms and thermodynamics. React. Funct. Polym., 118, 42–50.
[46] Bruckmann FS, Schnorr C, Oviedo LR, Knani S, Silva LFO, Silva WL, Dotto GL, Bohn Rhoden CR. (2022). Adsorption and Photocatalytic Degradation of Pesticides into Nanocomposites: A Review. Molecules.27(19), 6261. doi: 10.3390/molecules27196261.
[47] Haleem A, Shafiq A, Chen SQ, Nazar M. (2023). A Comprehensive Review on Adsorption, Photocatalytic and Chemical Degradation of Dyes and Nitro-Compounds over Different Kinds of Porous and Composite Materials. Molecules. 28(3),1081. doi: 10.3390/molecules28031081.
[48] Ćwieląg-Piasecka I. (2023). Soil Organic Matter Composition and pH as Factors Affecting Retention of Carbaryl, Carbofuran and Metolachlor in Soil. Molecules. 28(14), 5552. doi: 10.3390/molecules28145552.
[49] Alluhaybi, A.A., Alharbi, A., Alshammari, F.F. & El-Desouky, M.G. (2023). Efficient Adsorption and Removal of the Herbicide 2,4-Dichlorophenylacetic Acid from Aqueous Solutions Using MIL-88(Fe)-NH2 ACS Omega8(43), 40775-40784. DOI: 10.1021/acsomega.3c05818.
[50] Kulaishina, S.A., Vedenyapinaa, M.D. and A. Yu. Kurmyshevaa, A.Yu. (2022). Influence of the Surface Characteristics of Activated Carbon on the Adsorption of Herbicides (A Review). olid Fuel Chemistry, 56(3), 181–198.
[51] Mane, P.V., Rego, R.M., Yap, P.L., Losic, D. & Mahaveer D. Kurkuri, M.D. (2024). Unveiling cutting-edge advances in high surface area porous materials for the efficient removal of toxic metal ions from water, Progress in Materials Science, 146, 101314, doi.org/10.1016/j.pmatsci.2024.101314.
[52] Satyam S, & Patra S. (2024). Innovations and challenges in adsorption-based wastewater remediation: A comprehensive review. Heliyon. 10(9), e29573. doi: 10.1016/j.heliyon.2024.e29573.
[53] Ajala OA, Akinnawo SO, Bamisaye A, Adedipe DT, Adesina MO, Okon-Akan OA, Adebusuyi TA, Ojedokun AT, Adegoke KA, Bello OS. (2023). Adsorptive removal of antibiotic pollutants from wastewater using biomass/biochar-based adsorbents. RSC Adv. 13(7), 4678-4712. doi: 10.1039/d2ra06436g.
[54] Theodorakopoulos, G. V., Papageorgiou, S. K., Katsaros, F. K., Romanos, G. E., & Beazi-Katsioti, M. (2024). Investigation of MO Adsorption Kinetics and Photocatalytic Degradation Utilizing Hollow Fibers of Cu-CuO/TiO2 Nanocomposite. Materials, 17(18), 4663. https://doi.org/10.3390/ma17184663.
[55] Muthamilselvi, P., Ashish, K., Ponnusamy, S.K. Dai Viet, N. Vo., Akash, B., Meenu, M.J. & Prabhakar S. (2021). Sustainable adsorbents for the removal of pesticides from water: a review Environmental Chemistry Letters (2021) 19:2425–2463. doi.org/10.1007/s10311-021-01183-1.
[56] Al-Farttoosy, A.H. (2021). Adsorption-Desorption, and Kinetic Study of Diazinon by Batch Equilibrium Nat. Volatiles & Essent. Oils, 8(6), 4933-4939.
[57] Garba, Z.N., Abdullahi, A.K., Haruna, A. & Gana, S.A. (2021). Risk assessment and the adsorptive removal of some pesticides from synthetic wastewater: a review. Beni-Suef Univ J Basic Appl Sci10, 19, 1-18. doi.org/10.1186/s43088-021-00109-8.
[58] Ambursaa, M.M., Rabiub, A.K., Adebayoc, S.K., Bello, A. (2022). Adsorption of Pesticides from Aqueous Solution using Kinkeliba (Combretum micranthum G.) Derived Activated Carbon. International Journal of Sciences: Basic and Applied Research (IJSBAR) 63(2), 308-319.
[59] Amutova, F., Jurjanz, S., Akhmetsadykov, N., Kazankapova, M., Razafitianamaharavo, A., Renard, A., Nurseitova, M., Konuspayeva, G. & Delannoy, M. (2023). Adsorption of organochlorinated pesticides: Adsorption kinetic and adsorption isotherm study, Results in Engineering, 17, 100823, doi.org/10.1016/j.rineng.2022.100823.
[60] Ahmad F.A. (2023) The use of agro-waste-based adsorbents as sustainable, renewable, and low-cost alternatives for the removal of ibuprofen and carbamazepine from water. Heliyon. 9(6):e16449. doi: 10.1016/j.heliyon.2023.e16449.
[61] Bankole D. T., Oluyori A. P. & Inyinbor A. A. (2023) The removal of pharmaceutical pollutants from aqueous solution by Agro-waste. Arab. J. Chem. 2023,16.

[62] Tchakala, I., Bawa, L.M., Kodom, T., Djaneye-Boundjou, G., Doni, K.V. and Nambo, P. (2014). Kinetics of the Adsorption of Anionic and Cationic Dyes in Aqueous Solution by Low-Cost Activated Carbons Prepared from Sea Cake and Cotton Cake. Am. Chem. Sci. J., 4(1), 38-57.
[63] Zahaf, F., Dali, N., Marouf, R. and Ouadjenia, F. (2015). Removal of a textile dye by pillared clay. International Journal of Chemical and Environmental Engineering 6(1), 11-14.